

## REVIEW

# Aggregation-induced emission biomarkers for early detection of orthopaedic implant failure

Javad Tavakoli<sup>1,2</sup>  | Qi Hu<sup>3</sup>  | Joanne L. Tipper<sup>1,2</sup> | Youhong Tang<sup>3</sup> 

<sup>1</sup>Department of Biomedical Engineering, School of Engineering, RMIT University, Melbourne, Victoria, Australia

<sup>2</sup>School of Biomedical Engineering, Faculty of Engineering and IT, University of Technology Sydney, Sydney, New South Wales, Australia

<sup>3</sup>Institute for NanoScale Science and Technology, Medical Device Research Institute, College of Science and Engineering, Flinders University, Adelaide, South Australia, Australia

**Correspondence**

Javad Tavakoli, Department of Biomedical Engineering, School of Engineering, RMIT University, Melbourne, Victoria 3000, Australia. Email: [javad.tavakoli@rmit.edu.au](mailto:javad.tavakoli@rmit.edu.au)

Youhong Tang, Institute for NanoScale Science and Technology, Medical Device Research Institute, College of Science and Engineering, Flinders University, Adelaide, South Australia 5042, Australia.

Email: [youhong.tang@flinders.edu.au](mailto:youhong.tang@flinders.edu.au)

**Abstract**

In recent years, the substantial increase in total joint replacements for treating degenerative joint disease has heightened concerns regarding implant loosening and failure. This is especially critical as more young patients are undergoing both initial and subsequent joint replacement procedures. These complications often necessitate additional revision surgeries. Unfortunately, current clinical practices lack effective methods for the early detection of implant failure, and there is a noticeable absence of strategies utilizing molecular markers to identify post-surgery implant issues. This article critically assesses the potential of aggregation-induced emission (AIE) biomarkers in detecting molecular markers relevant to implant failure. It begins by outlining the pathogenesis of implant loosening and identifying pertinent molecular markers. The study then delves into how AIE luminogens (AIEgens) can play a crucial role in detecting processes such as osteogenesis and osteoclastogenesis. Notably, it discusses the utilization of AIEgens in detecting key molecular markers, including TNF- $\alpha$ , osteocalcin, and urinary N-terminal telopeptide. The prospect of AIE biomarkers for the early detection of bone loss and implant failure presents a promising avenue for enhancing our understanding of skeletal health and improving clinical outcomes through timely intervention and personalized treatment approaches. Ongoing research and development in this area are crucial for translating AIE-based technologies into practical tools for optimizing bone health management.

**KEYWORDS**

aggregation-induced emission, biomarkers, early detection, implant failure, orthopaedic implants, osteolysis

**Abbreviations:** 6-TAMRA, 6-carboxytetramethylrhodamine; Ada, Adalimumab; AIEgens, Aggregation-induced emission fluorogens; ALP, Alkaline phosphatase; BODIPY, Boron-dipyromethene; C2 linker, C2 indicates a short two-carbon linker; CBT motif, Cysteine-boronate transition state motif; CGPLGVRGK-BHQ3, Peptide-BHQ with C, G, P, L, V, R, and K representing cysteine, glycine, proline, leucine, valine, arginine, and lysine, respectively; Cit, Citrulline; CK, Cathepsin K; CyA-P-CyB, Two cyanine moieties linked via a cathepsin B-activated peptide (Gly-Phe-Leu-Gly); Cys, Cysteine; DHXP, 2',3'-Dideoxy-7,8-dihydro-8-oxoguanosine 5'-Triphosphate; DMEM, Dulbecco's modified eagle medium; ELISA, Enzyme-linked immunosorbent assay; FRET, Förster resonance energy transfer; GFLG, Gly-Phe-Leu-Gly; HAp, Hydroxyapatite; HCy, Hemicyanine; IL, Interleukin; MAL, Maleimide; MC-3T3-E1, Mouse Calvaria 3T3-E1; MMPs, Matrix metalloproteinases; NIR, Near-infrared; OPG, Osteoprotegerin; PEG4, Polyethylene glycol (with 4 repeat units); PEI, Polyethyleneimine; PTB-EDTA, Phenol-2,4,6-tribenzoic acid-ethylenediaminetetraacetic acid; RANK, Receptor activator of nuclear factor Kappa-B; RANKL, Receptor activator of nuclear factor Kappa-B ligand; RGD, Arginine-glycine-aspartic acid; RNA, Ribonucleic acid; RT-qPCR, Reverse transcription quantitative polymerase chain reaction; TNF- $\alpha$ , Tumour necrosis factor- $\alpha$ ; TPE, Tetraphenyl ethene; TRAP, Tartrate-resistant acid phosphatase; TTQF, Threonine-threonine-glutamine-phenylalanine tetrapeptide sequence; UAG, Uridine-adenosine-guanosine; Val, Valine amino acid.

## 1 | INTRODUCTION

Total joint replacement, also known as total joint arthroplasty, aims to alleviate pain, restore mobility, and improve the overall quality of life for patients suffering from severe joint diseases. In recent years, the prevalence of total joint replacement to treat degenerative joint disease has increased tremendously due to longer life expectancies leading to the growth of the elderly population and the obesity epidemic. Additionally, advancements in surgical technologies and healthcare services have facilitated timely diagnosis and treatment leading to an increase in the number of joint replacement interventions. The incidence of total knee and hip replacements is estimated to rise by 601% and 137%, respectively, by the year 2030.<sup>[1]</sup> With the limitation of total joint implants to fully recapitulate the anatomy, physiology, biomechanical function and kinematics of their native counterparts, their clinical benefits may not be the best option for

This is an open access article under the terms of the [Creative Commons Attribution](https://creativecommons.org/licenses/by/4.0/) License, which permits use, distribution and reproduction in any medium, provided the original work is properly cited.

© 2024 The Author(s). *Aggregate* published by SCUT, AIEI, and John Wiley & Sons Australia, Ltd.

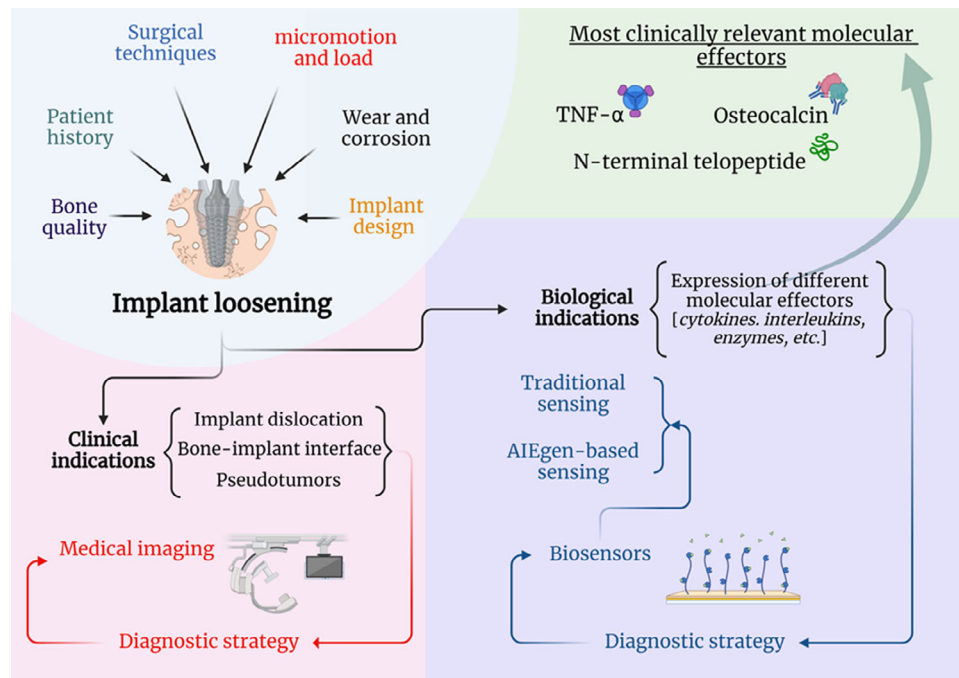


**FIGURE 1** Different factors (surgical techniques, patient bone quality, implant design, stress shielding, micromotion, and genetics) play a role in joint implant loosening including the associated indications (clinical and biological) leading to two different diagnostic strategies (medical imaging and biosensing). The development of new technologies, based on aggregation-induced emission luminogens (AIEgens), may improve the process enabling early detection of implant failure. The detection of clinically relevant molecular effectors should be the focus of future research to facilitate effective commercialisation in clinical practice (Created with BioRender.com).

younger more active patients. While challenges to developing innovative total joint implants to address the current problems still exist, concerns regarding implant loosening and failure leading to revision surgeries remain present. This issue is particularly significant as the demand for primary and revision total joint replacement surgeries in young patients is increasing.<sup>[2]</sup>

Different factors such as surgical techniques, patient bone quality, implant design, stress shielding, micromotion, and genetics play a role in the aseptic loosening of joint implants (Figure 1).<sup>[3,4]</sup> In addition, total joint replacement implants, consisting of metal and polymeric components creating metal-on-metal or metal-on-polymer articulations, are often exposed to different loading regimes and magnitudes; thus, generating wear debris. These wear particles can be from metals, bone cement, ceramics, and polymers with different characteristics such as morphology, size, and concentration. Wear particles exhibit different biological behaviour with smaller particles being more biologically active in terms of inducing inflammation and osteolysis leading to implant loosening.<sup>[5–7]</sup> Clinical imaging technologies such as radiography, CT, and MRI scans are the current diagnosis methodologies for the observation of implant dislocation as well as identification of gaps at the implant-bone interface (radiolucent lines) and pseudotumor; however, none of them are able to detect implant loosening at the early stage (Figure 1).<sup>[8,9]</sup> Timely detection of loosened implants is vital to prevent bone resorption and fracture and reduce the risks associated with late revision surgery. On the other hand, the early detection of osteolysis post-surgery may result in developing innovative strategies to employ molecular markers for future therapeutic advancement. For instance, expression of tumour necrosis factor- $\alpha$  (TNF- $\alpha$ ) is central to regulating

wear-induced osteolysis, and therefore, its inhibitors such as small interfering RNA and etanercept may offer viable treatment options to minimise the risk of implant failure.<sup>[10–12]</sup> From a biochemical point of view, the balance between the biological activities of osteoclasts and osteoblasts—the cells responsible for bone resorption and formation, respectively—controls bone remodelling. If the balance is altered, implant loosening is highly likely to occur.<sup>[13]</sup> The pathogenesis of osteolysis encompasses the sequence of biological events and mechanisms leading to the secretion of different molecular effectors including proinflammatory cytokines TNF- $\alpha$  and interleukins (e.g., IL-1 $\beta$ , IL-1, IL-6, IL-18), enzymes (e.g., matrix metalloproteinase 1, 2, 3, 9, 10, as well as alkaline phosphate and cathepsin), and osteoprotegerin.<sup>[14–18]</sup> Therefore, developing biomarkers to detect these molecular effectors from urine or serum samples may lead to the generation of advanced and non-invasive technologies crucial for early detection of implant loosening.<sup>[19–23]</sup>

Different methodologies and biosensing platforms have been used to detect molecular effectors associated with bone remodelling and osteolysis. Traditional electrochemistry and immunohistochemistry approaches for the detection of these molecular effectors require expensive biological optimisations, which are often time-consuming and suffer from poor stability and relatively long incubation times.<sup>[24–27]</sup> Enzyme-linked immunosorbent assay (ELISA) has been the most widely used immunoassay technique for the detection of the abovementioned molecular effectors; however, the associated antibody immobilization and frequent washing steps have made the process highly challenging.<sup>[27–29]</sup> Advanced technologies such as molecular imprinting to create sensitive biosensors and detect different molecular effectors involve multiple steps that significantly reduce commercial

viability.<sup>[30]</sup> Techniques based on optical tracking of particle motions and the use of antibody sandwich configurations rely on the diffusivity, density, and functionalisation of antibodies for the detection of molecular effectors, which induces complexity.<sup>[31]</sup> The presence of toxic reagents and high background noise have been the limitations of electrochemical biosensors.<sup>[32,33]</sup> Photoelectrochemical biosensing platforms are better options in terms of operational simplicity, superior stability, ultra-high sensitivity, and minimal background signal; however, low conversion efficiency and limited range of applications are their major drawbacks.<sup>[34–36]</sup>

The recent discovery of aggregation-induced emission luminogens (AIEgens) has opened new avenues to develop innovative biomarkers that may address the current major disadvantages.<sup>[37–39]</sup> AIEgen-based biomarkers are not initially fluorescent; however, their emission properties become significant in the aggregated state.<sup>[40–42]</sup> The elevated emission efficacy, excellent photostability, and high detection sensitivity of AIEgens, compared to other fluorescent molecules, make them an excellent platform for detecting molecular effectors.<sup>[43–47]</sup> AIEgens offer a promising tool for advancing diagnostics, monitoring, and treatment in the orthopaedic field, addressing challenges in conditions like osteoporosis, inflammation, and bone fracture healing.<sup>[48–51]</sup> This advancement is based on developing biomarkers that can detect the activity of osteoporosis-associated enzymes (such as alkaline phosphatase; ALP) in blood serum,<sup>[52,53]</sup> identify osteoporotic bone defects,<sup>[48]</sup> measure bone density,<sup>[50]</sup> track bone marrow cells,<sup>[54,55]</sup> and monitor bone healing, fractures, and inflammation.<sup>[56–58]</sup> Recently, AIEgens have also been used to study inflammatory pathways and the formation of urate crystals leading to rheumatoid arthritis.<sup>[59–61]</sup> Therefore, the first aim of the current study was to review and clarify the role of AIEgens in the monitoring of osteogenesis and osteolysis, the biological processes that are highly related to bone formation and bone resorption leading to implant loosening. The second aim of the current study was to explore the application of AIEgens in the detection of specific cytokines including TNF- $\alpha$ , osteocalcin and urinary N-terminal telopeptide. This aim, in particular, draws attention to developing novel AIEgen-based biomarkers that are highly clinically relevant leading to the generation of commercially viable biomarkers crucial for the early detection of implant failure.<sup>[62,63]</sup> A recent systematic review revealed that amongst different molecular effectors, the concentration of TNF- $\alpha$  and osteocalcin was significantly lower in stable compared with loosened implants.<sup>[64]</sup> Moreover, the concentration of urinary N-terminal telopeptide was substantially higher in patients with loosened joint implants.<sup>[64]</sup>

To the best of our knowledge, comprehensive research to identify the use of AIEgens for early detection of joint implant loosening and failure is yet to be conducted. A thorough search was performed through scientifically reputable databases, including PubMed, and Web of Science, from 2010 to 2024, using relevant keywords comprising “aggregation-induced-emission” combined with “osteogenesis”, “osteoclastogenesis”, “osteolysis”, “TNF- $\alpha$ ”, “osteocalcin”, and “urinary N-terminal telopeptide” with and without “joint implant”. Additionally, the bibliographies of identified studies were examined for additional relevant research.

## 2 | PATHOGENESIS OF JOINT IMPLANT LOOSENING

A healthy bone continuously undergoes a process of remodelling, where old bone is resorbed by osteoclasts, and new bone is formed by osteoblasts. Therefore, the relevant molecular effectors are actively produced and collectively contribute to the dynamic process of bone remodelling including synthesis, mineralisation, and resorption of bone matrix. In conditions of chronic inflammation or in the presence of different stimulators (such as wear particles from joint implants), elevated levels of the molecular effectors may indicate increased bone resorption, which can be associated with conditions such as osteoporosis or implant loosening.<sup>[65]</sup> Understanding the physiology of bone remodelling, osteoclastogenesis in particular, is central to understanding osteolysis associated with joint implants. Osteoclastogenesis, a process by which osteoclasts are formed and activated, is central to bone remodelling and maintenance of bone integrity.<sup>[13]</sup> Briefly, receptor RANK ligand (RANKL), a cytokine produced by osteoblasts, stimulates the differentiation and activation of osteoclasts. When RANKL binds to its receptor RANK on the surface of osteoclast precursors, it triggers intracellular signalling pathways that promote osteoclast formation and activity (Figure 2A). On the other hand, osteoprotegerin (OPG)—a glycoprotein that plays a crucial role in regulating bone metabolism—is produced by osteoblasts and its primary function is to regulate bone remodelling by acting as a decoy receptor of RANKL.<sup>[66]</sup> Therefore, OPG acts as a competitive inhibitor by binding to RANKL and preventing it from binding to RANK, thereby inhibiting osteoclast formation and activity. By regulating the balance between RANKL and OPG, the body can maintain bone homeostasis and prevent excessive bone resorption, which is essential for maintaining bone strength and integrity. Dysregulation of the RANKL/OPG ratio can lead to bone disorders leading to implant failure.<sup>[66]</sup> Within this intracellular signalling pathway, several molecular effectors play a critical role. Cytokines such as TNF- $\alpha$  and interleukin-1 $\beta$  (IL-1 $\beta$ ) stimulate RANKL expression (Figure 2B).<sup>[67]</sup> TNF- $\alpha$ , a pro-inflammatory cytokine produced by immune cells and other cell types, has been shown to enhance the expression of RANKL in osteoblasts. This creates a positive feedback loop whereby TNF- $\alpha$  stimulates the production of RANKL, further promoting osteoclastogenesis and bone resorption.<sup>[67]</sup> The combined actions of RANKL and TNF- $\alpha$  create a synergistic effect on osteoclastogenesis. TNF- $\alpha$  enhances the responsiveness of osteoclast precursors to RANKL, leading to increased osteoclast formation and activity (Figure 2B). Dysregulation of the RANKL/TNF- $\alpha$  feedback loop can have pathological consequences in conditions associated with excessive bone resorption where elevated levels of TNF- $\alpha$  and RANKL contribute to increased osteoclast activity and bone loss.<sup>[68]</sup> Mature and proliferated osteoblasts express tartrate-resistant acid phosphatase and cathepsin K, two enzymes that are central to osteolysis.

Amongst different molecular effectors TNF- $\alpha$ , osteocalcin, and urinary N-terminal telopeptides are key molecular effectors, the detection of these in body fluids may lead to early detection of joint implant loosening.<sup>[26]</sup> Osteocalcin is a major non-collagenous protein which is produced

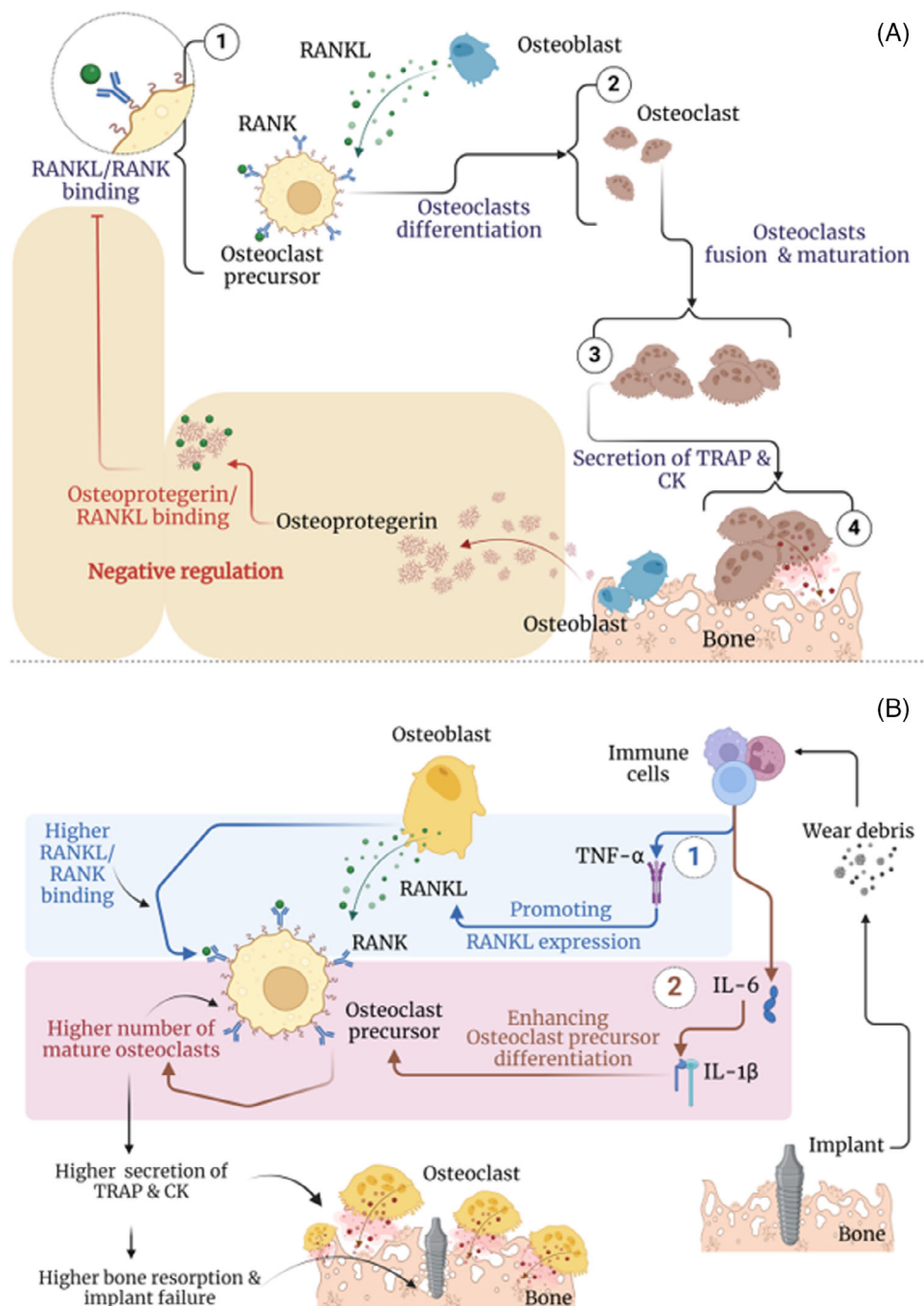


**FIGURE 2** (A) Osteoclastogenesis biological process indicates critical pathways for the formation of osteoclasts. (B) Pathogenesis of bone resorption and implant failure emphasizing the role of cytokine (TNF- $\alpha$ ) and interleukin (IL-1 $\beta$  and IL-6). The secretion of TNF- $\alpha$  by immune cells promotes RANKL expression leading to the formation of a higher number of mature osteoclast and a higher concentration of tartrate-resistant acid phosphatase (TRAP) and Cathepsin K (CK) at the bone-implant interface. Additionally, pro-inflammatory TNF- $\alpha$  and IL-6 can induce the production of IL-1 $\beta$  which acts directly on osteoclast precursor cells to enhance their differentiation and activation (Created with BioRender.com).

by osteoblast cells and is responsible for bone formation including bone metabolism and mineralization. TNF- $\alpha$  is a signalling protein (cytokine) which is involved in the regulation of inflammatory and immune responses within the body. Urinary N-terminal telopeptides are fragments of collagen molecules that are released during the breakdown of bone tissue, particularly during the resorption phase of bone remodelling. TNF- $\alpha$  contributes to implant loosening through different pathways including inflammation, bone resorption, matrix degradation, osteoblast function, osseointegration, and angiogenesis.<sup>[69–71]</sup> TNF- $\alpha$  stimulates the activation and differentiation of osteoclast cells responsible for bone resorp-

tion. Increased osteoclast activity leads to the breakdown of bone tissue around the implant, resulting in osteolysis and implant loosening.<sup>[69]</sup> Moreover, it promotes the production of matrix metalloproteinases (MMPs), enzymes involved in the degradation of extracellular matrix components, including collagen and proteoglycans.<sup>[70]</sup> MMPs contribute to the destruction of the bone-implant interface and the development of peri-implant osteolysis.<sup>[72]</sup>

TNF- $\alpha$  can inhibit the function of osteoblasts, cells responsible for bone formation; thus, limiting bone remodelling and leading to bone loss and implant instability.<sup>[73]</sup> Increasing the activation of osteoclasts and the inhibition of osteoblast

biological activity alters the bone resorption-formation balance and interferes with the process of osseointegration leading to implant loosening over time. Angiogenesis in periprosthetic tissue, formation of new blood vessels, can be dysregulated due to TNF- $\alpha$  hyperactivity contributing to tissue inflammation and bone remodelling abnormalities, further promoting implant loosening.<sup>[74]</sup> The relationship between osteocalcin level and implant loosening is not well-established and the associated mechanistic pathways are not clear. Implant loosening often triggers increased bone turnover and remodelling around the implant site. Osteocalcin, as a marker of bone turnover, may reflect this increased activity. Clinical studies examining bone metabolism around loosened implants have reported a higher osteocalcin level because of increased bone remodelling.<sup>[64,75]</sup> On the other hand, the release of inflammatory mediators and cytokines, due to wear debris or implant instability, in the periprosthetic environment stimulates bone turnover, potentially leading to elevated osteocalcin and urinary N-terminal telopeptides levels.<sup>[76,77]</sup>

### 3 | AGGREGATION-INDUCED EMISSION LUMINOGENS AND OSTEOGENESIS

Osteogenesis refers to the process of bone formation or the creation of new bone tissue. AIE biomarkers in this category are often able to inform the formation of new bone or osteoblast activity; hence, indirectly addressing bone loss. A recent study developed a highly soluble fluorescent molecule; an AIE-active tetraphenylthene (TPE) and benzothiadiazole containing conjugated polymer with ethylenediaminetetraacetic acid moiety (PTB-EDTA) exhibiting AIE characteristics. The ability of the AIEgen to adhere to osteogenic-differentiated cells leads to a gradual increase in fluorescence property as osteogenic differentiation progresses. PTB-EDTA displays maximum absorption and emission peaks at 429 and 594 nm, respectively, with a considerable Stokes shift of 165 nm, high quantum yield (approximately four-fold), and excellent biocompatibility making it suitable for bioimaging and sensing applications. The authors have compared this AIEgen with various osteogenic markers such as mRNAs by RT-qPCR, and have shown that PTB-EDTA could selectively illuminate osteoblast differentiation without interfering with osteogenic differentiation.<sup>[78]</sup> A water-soluble iridium (III) complex (Ir-BP2) serving as an AIE-active staining agent for bone matrix analysis has been developed recently. This has been made through adding phosphonate groups to the Ir-BP2 molecule enabling the formation of selective binding with bone component hydroxyapatite. With excellent biosafety characteristics, a prolonged lifetime, and high accuracy in staining calcium deposits, the AIE molecule was not only able to monitor the proliferation and differentiation of preosteoblast MC-3T3-E1 cells in real-time but also was capable of illuminating bone microstructure including microfractures.<sup>[50]</sup> In this study, Ir-BP2 was sprayed over the vertebrae in the spine to diagnose eosinophilic granuloma. In vertebral eosinophilic granuloma, Langerhans cells accumulate and form granulomas within the spine bone tissue increasing the risk of pathological fractures (Figure 3).

In another study, a dual-purpose near-infrared (NIR) light-activated AIEgen was developed enabling both remote control of cell differentiation and real-time monitoring of the process.<sup>[79]</sup> The biomarker was developed by encapsulating the photoactivatable caged compound (4,5-dimethoxy-2-nitroacetophenone/siRNA) and integrating it with an MMP13 cleaved imaging peptide-tetraphenyl ethene (TPE) unit, which was conjugated with mesoporous silica nanoparticles. Linking the AIEgen to silica nanoparticles using the MMP13-sensitive peptide in this research, enabled the release of AIEgen triggered by MMP13 through the cleavage of the linker peptide. As a result, the aggregation of released AIEgen exhibited a strong fluorescence signal at a 560 nm. Since the expression of MMP-13, a critical molecular effector for bone remodelling, is relevant to stem cell osteogenic differentiation, this AIEgen was effective in monitoring the differentiation process. Additionally, this study showed that upon NIR excitation the up-converted UV from mesoporous silica nanoparticles initiated the activation and release of the siRNA intracellularly leading to gene knockdown and effective induction of stem cell differentiation.<sup>[79]</sup> A similar strategy was used to prepare and engineer a photo-responsive nanoplatform based on up-conversion nanoparticles for near-infrared light-mediated control of intracellular icariin release, aimed at regulating the osteogenic differentiation of stem cells for osteoporosis treatment. Nanoparticles in this study were linked with photocaged and PEG linkers, 4-(hydroxymethyl)-3-nitrobenzoic acid and OH-PEG4-MAL, respectively. The nanoparticles were then conjugated with cap  $\beta$ -cyclodextrin and RGD-targeted peptide/matrix metalloproteinase 13; hence an MMP13-sensitive peptide-BHQ (CGPLGVRGK-BHQ3) was developed. Upon exposure to 980 nm NIR light, the upconverted UV emitted from the nanoparticles triggered the cleavage of cap  $\beta$ -cyclodextrin, leading to intracellular icariin release. This process induces osteogenic differentiation leading to the treatment of osteoporosis. Simultaneously, MMP13 that was generated during the osteogenic differentiation led to MMP13-sensitive peptide cleavage via removing BHQ and restoring the fluorescence of nanoparticles. This enabled real-time detection of osteogenic differentiation and assessment of the efficacy of the osteoporosis treatment.<sup>[80]</sup>

Alkaline phosphatase (ALP) plays a critical role as a monophosphate hydrolase in cell mineralisation and osteogenic differentiation. ALP is essential in bone formation through its roles in mineralization, matrix vesicle regulation, and induction of osteogenic genes. Its activity is a key indicator of osteogenic differentiation, making it an important enzyme in both research and clinical diagnostics related to bone health and regeneration. Only one study was found that specifically monitored ALP activity in living stem cells to detect osteogenic differentiation. In this study, three phosphorylated tetraphenylethylene (TPE) AIEgens (TPE-PA, TPE-2PA, and TPE-4PA) with varying numbers of  $-\text{PO}_3\text{H}_2$  group were synthesised. It was shown that both TPE-PA and TPE-2PA molecules exhibited high sensitivity to ALP in aqueous solutions through ALP accelerating hydrolysis of  $-\text{PO}_3\text{H}_2$  groups leading to the aggregation of the AIEgen (Figure 4A). However, only TPE-2PA demonstrated excellent cell penetrability and a high fluorescence signal-to-noise ratio during osteogenic differentiation in living cells.<sup>[81]</sup>

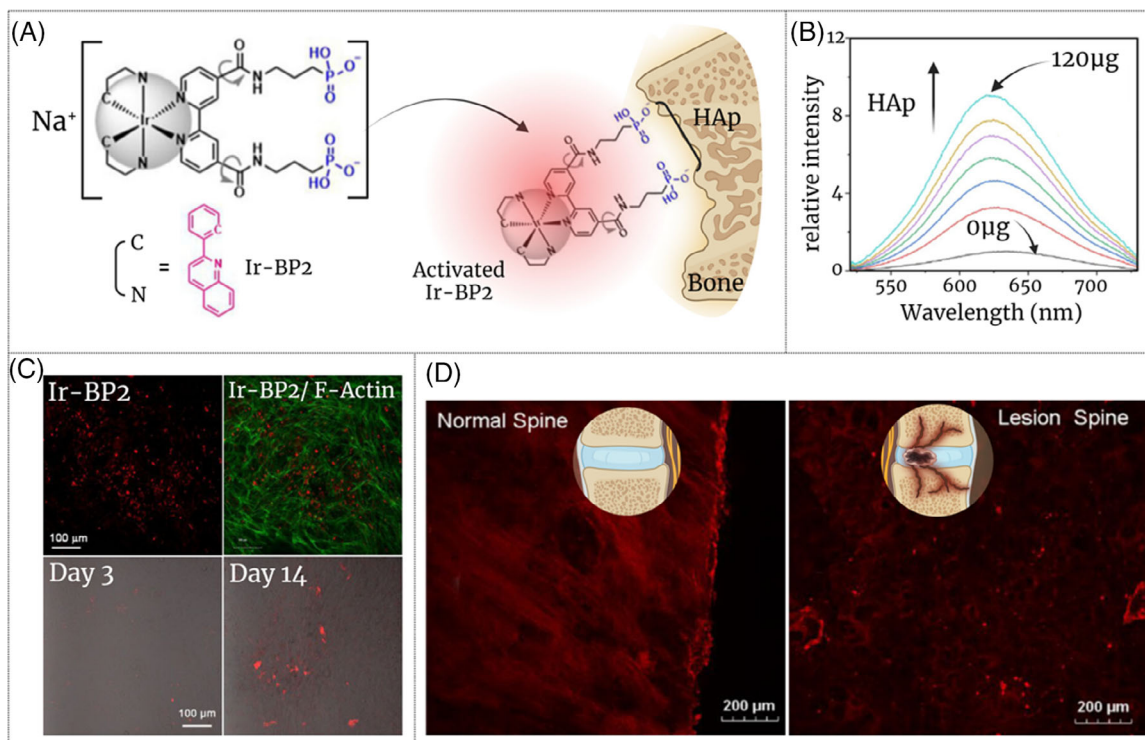


**FIGURE 3** (A) Chemical structure of Ir-BP2 and its immobilization on the bone surface via phosphonate- $\text{Ca}^{2+}$  chelation reaction leading to AIE activation. (B) Emission spectra of Ir-BP2 biomarker, titrated with Tris-HCl buffer containing Hydroxyapatite (HAp) particles. (C) Visualisation of osteogenesis differentiation of MC-3T3-E1 cells after 14 days indicating the capability of the AIEgen to bind with HAp produced by the cells (top) and confocal microscopy images of MC-3T3-E1 cells cultured with Ir-BP2 (20  $\mu\text{M}$ ) at day 3 and 14. (D) Diagnosis of spinal eosinophilic granuloma using Z-stacking imaging technique and ex-vivo samples after being spray-coated with prepared Ir-BP2.<sup>[50]</sup> Adapted with permission.<sup>[50]</sup> Copyright 2023, open access under CC by 4.0 DEED.

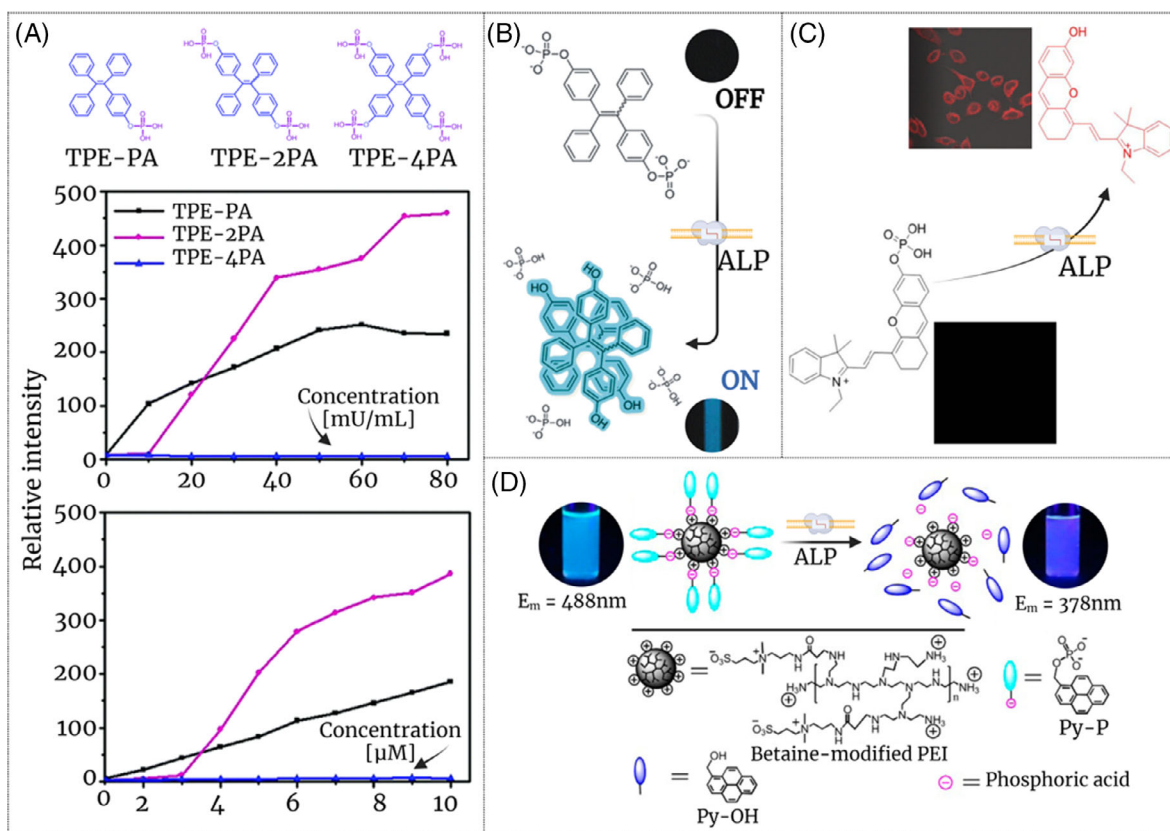


**FIGURE 4** (A) The chemical structures of three phosphorylated tetraphenylethylene (TPE) molecules (TPE-PA, TPE-2PA, and TPE-4PA) and their fluorescence spectra in the presence of different concentrations of ALP.<sup>[81]</sup> Adapted with permission.<sup>[81]</sup> Copyright 2012, Royal Society of Chemistry. (B) The turn-on fluorescent molecule based on TPE to monitor the activity of ALP.<sup>[82]</sup> Adapted with permission.<sup>[82]</sup> Copyright 2013, American Chemical Society. (C) Real-time monitoring of ALP activity using DHXP, a derivative of 3-dihydro-1H-xanthene-6-ol molecule with a phosphatase reactive site.<sup>[83]</sup> Adapted with permission.<sup>[83]</sup> Copyright 2017, American Chemical Society. (D) Schematic illustration, the chemical structure, and fluorescent properties of benzopyrene biomarker in response to ALP.<sup>[84]</sup> Adapted with permission.<sup>[84]</sup> Copyright 2014, American Chemical Society.

Several studies have employed AIEgens to monitor ALP activity in serum and cells.<sup>[82–84]</sup> While these studies did not specifically target ALP activity resulting from osteogenic differentiation, they developed AIE biomarkers characterized by simple structure, a one-step synthesis process, high sensitivity for detecting ALP at low concentrations, and high accuracy in measuring ALP activity. These attributes suggest that further research could expand their clinical applications to include the detection and monitoring of ALP activity in the osteogenesis process. A turn-on AIE biomarker, based on TPE with two phosphate groups featuring AIE properties, was developed to detect ALP activity. The phosphorylation of TPE served dual purposes: providing specific sites for subsequent ALP catalysis and transforming the parent structure into a water-soluble species, rendering the AIEgen nearly non-fluorescent in water. Upon the addition of ALP, the phosphate groups were cleaved, yielding insoluble TPE with two hydroxyl groups (TPE-2OH), which could aggregate to produce intense fluorescence emission (Figure 4B). The detection limit was found to be  $0.2 \text{ U L}^{-1}$  in Tris buffer solution with a linear quantification range of  $3\text{--}526 \text{ U L}^{-1}$  (with a linear range of up to  $157 \text{ U L}^{-1}$  for a dilute serum).<sup>[82]</sup>

In another study, a ratiometric fluorescent molecule with AIE feature and enhanced permeability and retention characteristics was developed for ALP activity assay by simple modification of 2'-hydroxychalcone.<sup>[85]</sup> It was shown that upon exposure to ALP, the emission spectrum of the AIEgen shifted from yellow-green to red allowing the monitoring of ALP activity within a concentration range of  $0\text{--}150 \text{ mU mL}^{-1}$  (detection limit of  $0.15 \text{ mU mL}^{-1}$ ).<sup>[85]</sup> A near-infrared AIEgen based on a derivative of 3-dihydro-1H-xanthen-6-ol (DHX) which contained a phosphatase reactive site (DHXP) was synthesised and characterised for real-time monitoring of ALP activity (Figure 4C). This study demonstrated that the AIEgen exhibited a remarkable up to 66-fold increase in fluorescence intensity upon interaction with ALP with a detection limit of  $0.07 \text{ U L}^{-1}$ . While this study did not use the biomarker to detect ALP originated by osteogenic differentiation, it was found highly effective in monitoring the ALP activity produced during Hella cell proliferation and endogenous ALP predominant in a mouse model.<sup>[83]</sup> Utilising benzopyrene, an AIEgen comprised two components: the positively charged polyethyleneimine (PEI) and the negatively charged pyrene derivative, was synthesized which enabled the ratio detection of ALP levels (detection limit of  $0.1 \text{ U mL}^{-1}$ ) in human serum samples due to enzymatic reactions (Figure 4D).<sup>[84]</sup>

#### 4 | AGGREGATION-INDUCED EMISSION LUMINOGENS AND OSTEOCLASTOGENESIS

Osteoclastogenesis is the process by which osteoclasts, specialized cells responsible for bone resorption, are formed from precursor cells. Cathepsins, a group of lysosomal proteases, play a critical role in various physio-pathological processes and are key enzymes involved in the degradation of bone matrix proteins during osteoclast-mediated bone resorption.<sup>[86,87]</sup> In particular, cathepsin K is predominantly expressed in osteoclasts and is one of the most important cathepsins involved in bone resorption. It is responsible for

degrading type I collagen, the main structural protein in bone, and other matrix proteins within the bone matrix. Cathepsin K plays a critical role in the formation of the resorption lacuna, the space created by osteoclasts during bone resorption. An increase in the concentration of cathepsin K at the implant site can lead to the loosening and consequent failure of the implant.<sup>[88]</sup> On the other hand, cathepsin B participates in the degradation of extracellular matrix components and facilitates the migration and fusion of osteoclast precursor cells during osteoclastogenesis. Cathepsin B regulates signalling pathways involved in osteoclast activation and bone resorption and modulates the activity of growth factors, cytokines, and cell surface receptors that regulate osteoclast function and the bone remodelling processes. Therefore, higher activity or concentration of cathepsin B may reflect early implant failure.<sup>[89]</sup>

Unfortunately, no studies have been published to date that focus on developing an AIE biomarker specifically designed to detect cathepsins secreted by osteoclasts in the context of implant failure studies. Although a series of cathepsin-activatable biomarkers have been developed recently, they either lack AIE characteristics or have been used for applications that are irrelevant to osteoclasts. For example, A TPE derivative (TPECM-2N<sub>3</sub>) biomarker, which was sensitive to cathepsin B, was synthesised for the targeted and image-guided photodynamic ablation of cancer cells.<sup>[90]</sup> The AIE molecule was composed of 4 components. The main molecular building blocks of the biomarker were a peptide substrate (Gly-Phe-Leu-Gly; GFLG) sensitive to cathepsin B, a fluorescent AIE molecule (TPECM-2N<sub>3</sub>), a hydrophilic linker containing three Asp (D) units, and an RGD-targeting moiety. The cathepsin B-mediated cleavage of the GFLG substrate initiates intensified fluorescence emitting an orange-red light in the aggregated state.<sup>[90]</sup> The AIE molecule exhibited a rapid, steady, and linear ( $R^2 = 0.99$ ) increase in fluorescence (35-fold in 60 min) upon the addition of cathepsin B, indicating its potential for quantifying the enzyme via measuring the fluorescent intensity change.

Investigating osteoclastogenesis by monitoring changes in the acidic microenvironment of bone can provide insights into osteoclast function. The fact that the osteoclast activity is higher in osteolysis was the core of a study where a bone-targeting molecular biomarker (TTQF-SO<sub>3</sub>) based on TTQF which is a donor-acceptor-donor-based NIR-II fluorophore (Figure 5A). The addition of functional amino groups to TTQF developed TTQF-NH<sub>2</sub>, and the subsequent sulfonation in the presence of 1,3-propanesultone led to the production of TTQF-SO<sub>3</sub>. With a dendritic molecular structure, TTQF-SO<sub>3</sub> exhibited high solubility ( $100 \text{ mg mL}^{-1}$ ) in aqueous media, displayed high affinity toward inorganic calcium salts, showed high optical stability (>14 days in DMEM), and was able to self-assemble to form ultra-small dots with 8.7 nm average size with absorption and emission peaks at 742 and 1064 nm, respectively, indicating a large Stokes shift. This study revealed a significant difference in the fluorescent properties of TTQF-SO<sub>3</sub> (three-fold higher) for healthy and osteoporotic bone in a mouse model 30 min after injection. Based on the higher accumulation of TTQF-SO<sub>3</sub> in osteoporosis mice which contain osteoclast precursors, this research suggested the AIEgen to be used for the monitoring of osteoclast activity and bone resorption imaging.<sup>[91]</sup>

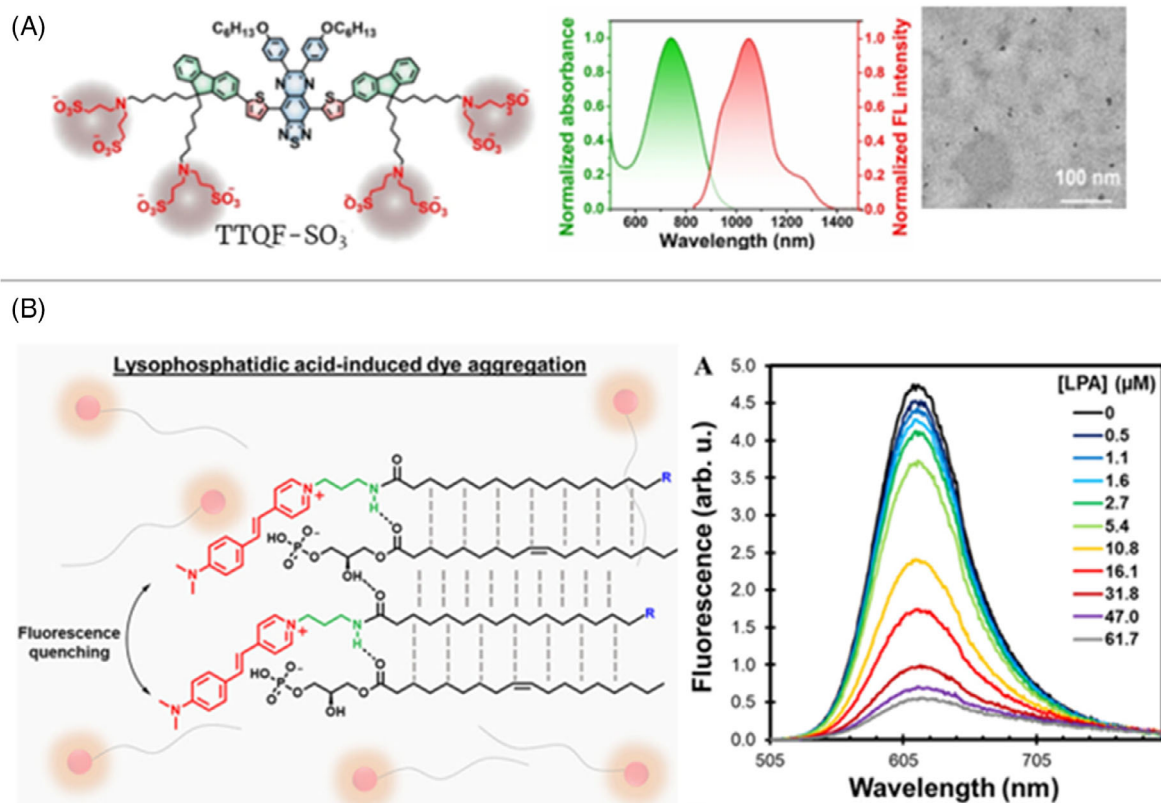


**FIGURE 5** (A) The chemical structure of TTQF-SO<sub>3</sub>, its fluorescent properties, and its TEM image.<sup>[91]</sup> Adapted with permission.<sup>[91]</sup> Copyright 2023, BMC Springer Nature; open access under a Creative Commons Attribution 4.0 International License. (B) Detection of lysophosphatidic acid (LPA) and the relevant ACQ mechanism.<sup>[92]</sup> Adapted with permission.<sup>[92]</sup> Copyright 2022, ACS Publications; open access under a Creative Commons Attribution 4.0 International License.

Lysophosphatidic acid, produced by osteoblasts, is a bioactive phospholipid that mediates intercellular signalling between osteoblasts and osteoclasts and induces pleiotropic effects on osteoclast activity and function.<sup>[92]</sup> A recent study developed a series of lysophosphatidic acid-sensitive fluorescent biomarkers, based on styrylpyridinium dyes, with aggregation-induced fluorescence quenching (Figure 5B). These biomarkers were produced by the addition of *N*-hydroxysuccinimide, silan, and azide groups to the dye structure. The focus of this study was to understand the effect of the molecular structure on the sensitivity and fluorescent properties, leading to the spectrophotometric characterization of the biomarkers. With the detection limits of nanomolar and excellent lysophosphatidic acid selectivity—even in the presence of ions and small molecules such as glycerol, ATP, sodium nitrate, sodium chloride, etc.—these biomarkers, while not directly discussed in the current research, were suggested to be used to investigate osteoclast activity.<sup>[93]</sup>

## 5 | AGGREGATION-INDUCED EMISSION LUMINOGENS AND DETECTION OF CLINICALLY RELEVANT MOLECULAR EFFECTORS

Recent studies have revealed that TNF- $\alpha$ , osteocalcin, and urinary N-terminal telopeptide are the most clinically relevant molecular effectors indicating implant loosening. It was reported that the concentrations of these molecular effectors have been significantly lower in stable

compared with loosened implants.<sup>[62–64]</sup> Different technological platforms such as electrochemical impedance spectroscopy, electrochemistry-based biosensors, enzyme-linked immunosorbent assay (ELISA), DNA aptamers, fibre optics, single molecule counting have been widely used for TNF- $\alpha$  detection; however, the relevant measurement techniques are often complicated and include complex design strategies.<sup>[94–97]</sup> Recently, a few studies have shown the capability of AIE-based biomarkers for TNF- $\alpha$  detection which holds significant promise for various biomedical applications, including disease diagnosis, drug screening, and biomarker profiling.<sup>[98]</sup> However, none were employed to directly detect TNF- $\alpha$  relevant to joint implant failure. The high sensitivity, selectivity, and real-time monitoring capabilities of AIE-based techniques enable the detection of low concentrations of TNF- $\alpha$  in complex biological samples, offering valuable insights into disease pathogenesis and therapeutic responses. A recent study has used the phenomenon of aggregation-caused quenching and developed a biomarker to detect TNF- $\alpha$ . The quenchbody biomarker was based on 6-TAMRA-C2-mal fluorescent dye whose fluorescent properties were recovered after being exposed to TNF- $\alpha$  molecules reaching the maximum intensity within 5 min (Figure 6A). With the limit detection of 0.123 ng mL<sup>-1</sup> (half-maximum effective concentration of 25 ng mL<sup>-1</sup>), a four-fold increase in the biomarker intensity was reported for 1  $\mu$ g mL<sup>-1</sup> concentration of TNF- $\alpha$ .<sup>[99]</sup> Briefly, two antigen-binding fragments of Adalimumab (Ada), a human monoclonal antibody that specifically binds to TNF- $\alpha$ , were prepared and both were chemically linked to 6-TAMRA-C2-maleimide and

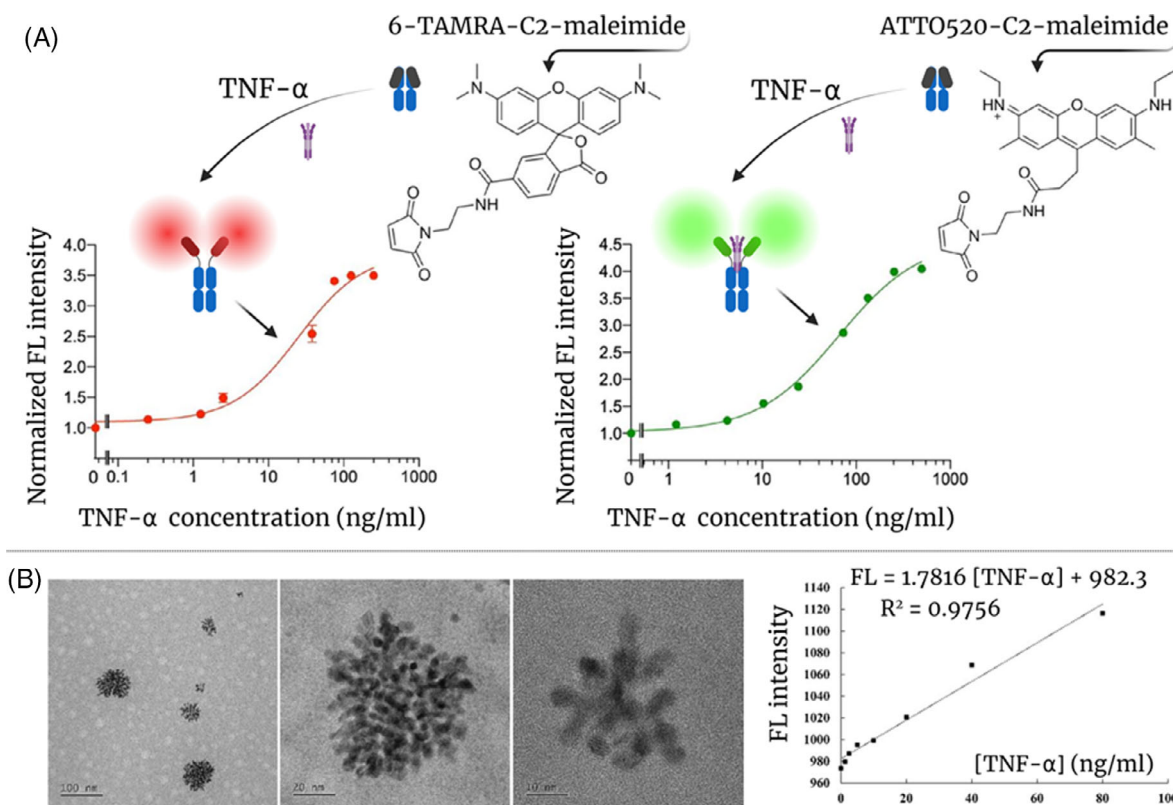


**FIGURE 6** (A) The fluorescent properties of TAMRA-conjugated-Ada antigen fragment AIE biomarkers upon being exposed to TNF- $\alpha$  with different concentrations.<sup>[99]</sup> Adapted with permission.<sup>[99]</sup> Copyright 2021, American Chemical Society; open access licensed under CC-BY-NC-ND-4.0. (B) TEM images of gold nanocluster system and its fluorescent response to TNF- $\alpha$  with different concentrations.<sup>[101]</sup> Adapted with permission.<sup>[101]</sup> Copyright 2024, Elsevier.

ATTO520-C2-maleimide molecules. Upon being exposed to TNF- $\alpha$  both biomarkers exhibited fluorescent properties with an increasing trend towards higher TNF- $\alpha$  concentrations (Figure 6A). With a similar approach, four different types of TAMRA-conjugated quench-bodies with different spacer lengths were shown to exhibit different fluorescent properties when were exposed to TNF- $\alpha$ . It was revealed that the longer spacer length led to a higher de-quenching leading to an increase of approximately four-fold in fluorescent relative intensity for all different concentrations of TNF- $\alpha$  ranging from  $1 \times 10^{-6}$  to  $1 \times 10^{-8}$  M.<sup>[100]</sup> A gold nanocluster system with fluorescent properties was shown to be sensitive enough to detect TNF- $\alpha$  where the higher concentrations (from 1.25 to 80 ng mL<sup>-1</sup>) resulted in higher fluorescent intensities (Figure 6B). A positive linear correlation between the concentration of TNF- $\alpha$  and fluorescent intensity (correlation coefficient = 0.975) was also reported for the AIEgen.<sup>[101]</sup>

Only a few studies have used Förster resonance energy transfer (FRET) phenomena to develop FRET-based DNA molecules—known as Quenchbodies—for the detection of osteocalcin.<sup>[102–104]</sup> A FRET molecule typically consists of two fluorophores: a donor and an acceptor. The donor fluorophore absorbs light at a specific wavelength and then transfers its energy to the acceptor fluorophore through non-radiative dipole-dipole coupling. This energy transfer occurs when the donor and acceptor fluorophores are in proximity often within several nanometres and results in a decrease in fluorescence from the donor and an increase in fluorescence from the acceptor.<sup>[105,106]</sup> The efficiency of energy transfer depends on the distance and orientation between the donor and acceptor fluorophores, making FRET molecules sensi-

tive to molecular conformational changes, protein–protein interactions, or changes in environmental conditions. Traditional antibody probes relying on a FRET mechanism, often suffer from limitations such as spectral overlap and photobleaching. To address these limitations, researchers recently introduced quench-based antibody biomarkers that utilize dye–dye interactions (mainly TAMRA) with enhanced antigen-dependent fluorescence to develop a series of novel-type antibody molecules with fluorescent properties called Ultra Q-bodies. The synthesis of the biomarkers was based on the incorporation of TAMRA-C6-fragment of antigen binding (Fab) complex into the H chain (Fd, V<sub>H</sub>-C<sub>H</sub>1) of Fab in response to a UAG codon in a cell-free translation system. These molecules utilised a quenching mechanism based on dye-dye interactions, leading to enhanced fluorescence in the presence of osteocalcin (approximately ten-fold). When the Ultra Q-bodies bound to osteocalcin, the dye-dye interactions were disrupted, resulting in enhanced fluorescence emission.<sup>[102–104]</sup> To date there has not been a study for the detection of urinary N-terminal telopeptide using AIEgens.

## 6 | AGGREGATION-INDUCED EMISSION LUMINOGENS AND POTENTIAL TREATMENT FOR LOOSENED JOINT IMPLANTS

Osteoporosis occurs when the creation of new bone does not keep up with the removal of old bone. This imbalance results in bones becoming weak and brittle. Implant failure and osteoporosis can be interrelated, especially

in scenarios where implants are used to stabilise bones weakened by osteoporosis. AIEgens in combination with microRNA approaches have shown promise in developing effective strategies that promote bone formation while inhibiting bone resorption.<sup>[49,107]</sup> A spherical nucleic acid was synthesized via a self-assembly process by using a pyridyl disulfide-terminated AIE molecule ((E)-1-(6-((tert-butoxycarbonyl) amino)hexyl)-4-(2-(9-ethyl-9H-carbazol-2-yl)vinyl)quinolin-1-ium bromide) as the hydrophobic core coupled with a thiolated-miRNA as the hydrophilic shell. Additionally, a VH6 aptamer was co-assembled with the prepared spherical nucleic acid facilitating miR-26 bone selective uptake. The integration of an AIE molecule, a CH6 aptamer and MiRNAs into a single nanoplateform enabled bone-targeted delivery of miR-26 with high efficiency and optimizing bone remodelling and healing while minimising adverse effects in non-skeletal tissues. By optimising bone anabolic action through targeting glycogen synthase kinase 3 beta in bone marrow mesenchymal stem cells and cellular communication network 2 in osteoclasts, the platform showed an excellent anti-osteoclastogenic properties. The use of AIE molecule, while facilitating the self-assembly of the platform, provided opportunities to monitor the relevant cellular uptake and associated lysosomal escape capacity.<sup>[49]</sup> Table 1 presents a summary of AIEgen biomarkers with potential application for early detection of joint implants loosening.

The high levels of reactive oxygen species (ROS), represented by hydrogen peroxide ( $H_2O_2$ ), at the implant site, are relevant to an uncontrolled inflammatory condition and strongly related to bone loss; hence, an indication of early implant failure.<sup>[118]</sup> Inflammation, ROS, and implant loosening are interconnected processes where persistent inflammation, driven by pro-inflammatory cytokines like TNF- $\alpha$ , IL-1 $\beta$ , and IL-6, leads to the generation of ROS by immune cells.<sup>[119–121]</sup> These ROS cause oxidative stress, damaging cellular components and promoting osteoclast activity, resulting in bone resorption. Key effectors such as MMPs, which degrade extracellular matrix, and the RANK/RANKL/OPG pathway, which regulates osteoclastogenesis, further contribute to the weakening of the bone-implant interface.<sup>[122]</sup> This interplay ultimately leads to implant loosening, exacerbated by both aseptic conditions and infections. While different AIE-based biomarkers have been developed for the detection of  $H_2O_2$ , they are unlikely to provide effective information about implant failure, since only chronic inflammation may lead to bone loss and implant failure.<sup>[123,124,47,125]</sup> Therefore, these type of AIE biomarkers were excluded from the current research; however, their theranostic properties may reduce inflammation while allowing monitoring of the process ensuring inflammation treatment.<sup>[126,127]</sup>

## 7 | FUTURE DIRECTION

The future of AIEgen-based biomarkers for early detection of bone loss and implant failure holds promise for advancing our understanding of skeletal health and improving clinical outcomes through early intervention and personalised treatment strategies. Continued research and development in this field are essential for translating AIE-based technologies into prac-

tical tools for improving bone health management. The focus of future studies should address the current limitations including the limited number of AIE biomarkers for the detection of clinically relevant molecular effectors. Additionally, no study has yet developed an AIE biomarker to specifically detect cathepsins secreted from osteoclasts (i.e., cathepsin K) for implant failure studies. Cathepsin K is predominantly expressed in osteoclasts and is one of the most important cathepsins involved in bone resorption. It is responsible for degrading type I collagen, the main structural protein in bone, and other matrix proteins within the bone matrix. Cathepsin K plays a critical role in the formation of the resorption lacuna, the space created by osteoclasts during bone resorption. An increase in the concentration of cathepsin K at the implant site can be attributed to its loosening and the consequent failure.

To further address the current gaps, several strategies can be proposed. One approach is to synthesize multi-component probes sensitive to the molecular effectors involved in osteogenesis and osteoclastogenesis processes. For example, the development of multicomponent biomarkers, with one component sensitive to the cathepsin enzyme, has been investigated in several recent studies.<sup>[108–110]</sup> However, the fluorescent molecules generated after cleavage lacked AIE properties. For instance, a near-infrared fluorescent biomarker (CyA-P-CyB) containing two cyanine moieties linked via a cathepsin B-activated peptide (Gly-Phe-Leu-Gly) was synthesised. CyA and CyB moieties serve as a fluorescent donor and a quencher, respectively. The biomarker remained non-fluorescent due to efficient Förster resonance energy transfer from CyA to CyB, while an intense NIR fluorescent emission was observed upon the cleavage of the peptide linker by cathepsin B (Figure 7A). This biomarker enabled the visualisation of cathepsin B activity and lysosome membrane permeabilization in cells.<sup>[108]</sup> In another study, a fluorescent molecule was developed based on a dipeptide substrate Val-Cit for cathepsin B-specific cleavage and a D-aminoluciferin moiety for bioluminescence generation. This study showed that caging the amino group of D-aminoluciferin by the carboxyl group of citrulline (Cit) during the synthesis of the molecule resulted in the inactivation of fluorescent properties; however, cathepsin cleavage of the Val-Cit substrate from Val-Cit-D-aminoluciferin produced free D-aminoluciferin inducing bioluminescence properties (Figure 7B). The associated bioluminescence characteristics were due to the catalysis of firefly luciferase (fLuc).<sup>[109]</sup> Hemicyanine (HCy), characterised by tuneable NIR absorption and emission driven by intramolecular charge transfer, has found extensive application in fluorescence imaging. HCy was recently used to develop biomarkers to detect the overexpressing of cathepsin B in vivo. The fluorescent molecules contained two peptide sequence components including HCy and Val-Cit and Gly-Phe-Leu-Gly as the specific moieties sensitive to cathepsin B. Since the amino group of HCy was caged by the moieties, the biomarkers exhibited no fluorescent properties in the absence of cathepsin B. Upon exposure to cathepsin, the cleavage HCy-Cit-Val and HCy-Gly-Leu-Phe-Gly that occurred resulted in the release of free HCy-NH<sub>2</sub> with activated fluorescent signals (Figure 7C).<sup>[110]</sup>

This strategy can be effectively used to develop highly efficient cathepsin-sensitive biomarkers if the linking components exhibit AIE properties after cleavage.<sup>[90]</sup> The increased and more stable fluorescence alongside higher sensitivity and

TABLE 1 List of biomarkers with potential application in the detection of joint implant loosening and failure.

Biomarkers for osteogenesis	
Probe	Description
PTB-EDTA	A highly soluble anion-conjugated polymer with AIE characteristics and the ability to adhere to osteogenic-differentiated cells. <sup>[78]</sup>
Ir-BP2	A water-soluble iridium (III) complex serving as an AIE-active staining agent for bone matrix analysis. <sup>[50]</sup>
4,5-dimethoxy-2-nitroacetophenone/siRNA-TPE	Cleavage via exposure to MMP13 leads to generating a strong fluorescence signal. <sup>[79]</sup>
4-(hydroxymethyl)-3-nitrobenzoic acid—OH-PEG4-MAL	An MMP13-sensitive compound to induce and detect osteogenic differentiation. <sup>[80]</sup>
Phosphorylated TPE (with varying numbers of —PO <sub>3</sub> H <sub>2</sub> group)	Detection of cell mineralization and osteogenic differentiation via monitoring the activity of alkaline phosphatase. <sup>[81]</sup>
TPE-2OH	Detection of osteogenic differentiation via monitoring the activity of alkaline phosphatase. <sup>[82]</sup>
2'-hydroxychalcone	Triggered by alkaline phosphatase, the emission spectrum of the biomarker shifted from yellow-green to red. <sup>[85]</sup>
3-dihydro-1H-xanthene-6-ol (DHX)	A 66-fold increase in fluorescence intensity upon interaction with Alkaline phosphatase. <sup>[83]</sup>
Polyethylenimine—benzopyrene	Detection of alkaline phosphatase levels (detection limit of 0.1 U mL <sup>-1</sup> ) in human serum. <sup>[84]</sup>
Biomarkers for osteoclastogenesis	
TPECM-2N <sub>3</sub>	Sensitive to cathepsin B. <sup>[90,108]</sup>
Val-Cit-D-aminoluciferin	Detection of cathepsin B through the production of D-aminoluciferin. <sup>[109]</sup>
Val-Cit-Hcy-Gly-Phe-Leu-Gly	Upon exposure to cathepsin B, the cleavage Hcy-Cit-Val and Hcy-Gly-Leu-Phe-Gly occurs resulting in the release of free Hcy-NH <sub>2</sub> with activated fluorescent signals. <sup>[110]</sup>
Rhodamine	The increase in the fluorescent intensity of rhodamine upon exposure to osteoclast acidic secretion (hydrochloric acid and proteases, such as cathepsin K) enabled the study of osteoclast activity. <sup>[111]</sup>
TTQF-SO <sub>3</sub>	Monitoring of osteoclast activity and bone resorption imaging. <sup>[91]</sup>
Styrylpyridinium—integrated with N-hydroxysuccinimide, Silan, and Azide groups	To monitor and detect the activity and production of lysophosphatidic acid; a bioactive phospholipid that mediates intercellular signalling between osteoblast and osteoclast. <sup>[92,93]</sup>
Cys(StBu)-Ala-Ala-Asn-Lys(FMBA)-CBT	To detect protease legumain, an endopeptidase that inhibits osteoclast formation and bone resorption. <sup>[112–114]</sup>
pH-sensitive biomarkers with bone-binding affinity	
BODIPY	Measuring pH variation associated with osteoclast activity enabling investigation of the mechanism of bone resorption. <sup>[115–117]</sup>
Clinically-relevant biomarkers (TNF- $\alpha$ and osteocalcin)*	
6-TAMRA-C2-maleimide	To detect TNF- $\alpha$ at a low concentration of 1 $\mu$ g mL <sup>-1</sup> . <sup>[99,100]</sup>
Gold nanocluster	To detect TNF- $\alpha$ at the concentration range of 1.25–80 ng mL <sup>-1</sup> . <sup>[101]</sup>
FRET-based DNA biomarkers	To detect osteocalcin with 10-fold enhancement of fluorescent properties in the presence of osteocalcin. <sup>[102–104]</sup>

\*None were employed to directly detect TNF- $\alpha$  relevant to joint implant failure.

\*No study was found for the detection of urinary N-terminal telopeptide using AIEgens.

lower detection limit resulting from aggregation makes this approach suitable for the clinical early diagnosis of osteoclastogenesis. The proposed strategy has been employed once to develop a cathepsin-activatable biomarker for applications that are irrelevant to osteoclasts.<sup>[90]</sup> Further research is needed to determine whether biomarkers developed using the proposed strategy can be utilized to monitor cathepsin enzymes during osteoclastogenesis and for the early detection of joint implant failure.

Another strategy is to develop AIE biomarkers sensitive to changes in the acidic microenvironment of bone, enabling the monitoring of osteoclast function. A key aspect of biomarker design should be their affinity for bone, making them suitable for in-situ detection of osteoclast activity and acid secretion. So far, the AIE community has developed several pH-sensitive AIEgens, primarily for pH-mediated tumour imaging and photodynamic therapy. However, their potential for analysing osteoclast activity has not yet been

explored. Valuable lessons can be drawn from traditional fluorescent dyes that have been developed using a similar strategy. For instance, rhodamine spirolactam-based dyes were developed for the detection of acidic microenvironments enabling the monitoring of osteoclast function. These probes were developed based on significant enhancement of the fluorescence response via electron-withdrawing *N*-alkyl substituents in the rhodamine. The increase in the fluorescence intensity of rhodamine upon exposure to osteoclast acidic secretions (hydrochloric acid and proteases, such as cathepsin K) enabled the study of osteoclast activity (mainly dynamics of osteoclast proton pumps) during bone resorption (Figure 8A). This study revealed that the accumulation of proton pumps appeared at the bone surface during acidic osteoclast bone resorption using a mouse model.<sup>[111]</sup> With a similar approach, several studies have developed small molecular pH-sensitive AIE biomarkers with bone-binding affinity through conjugating boron dipyrromethene

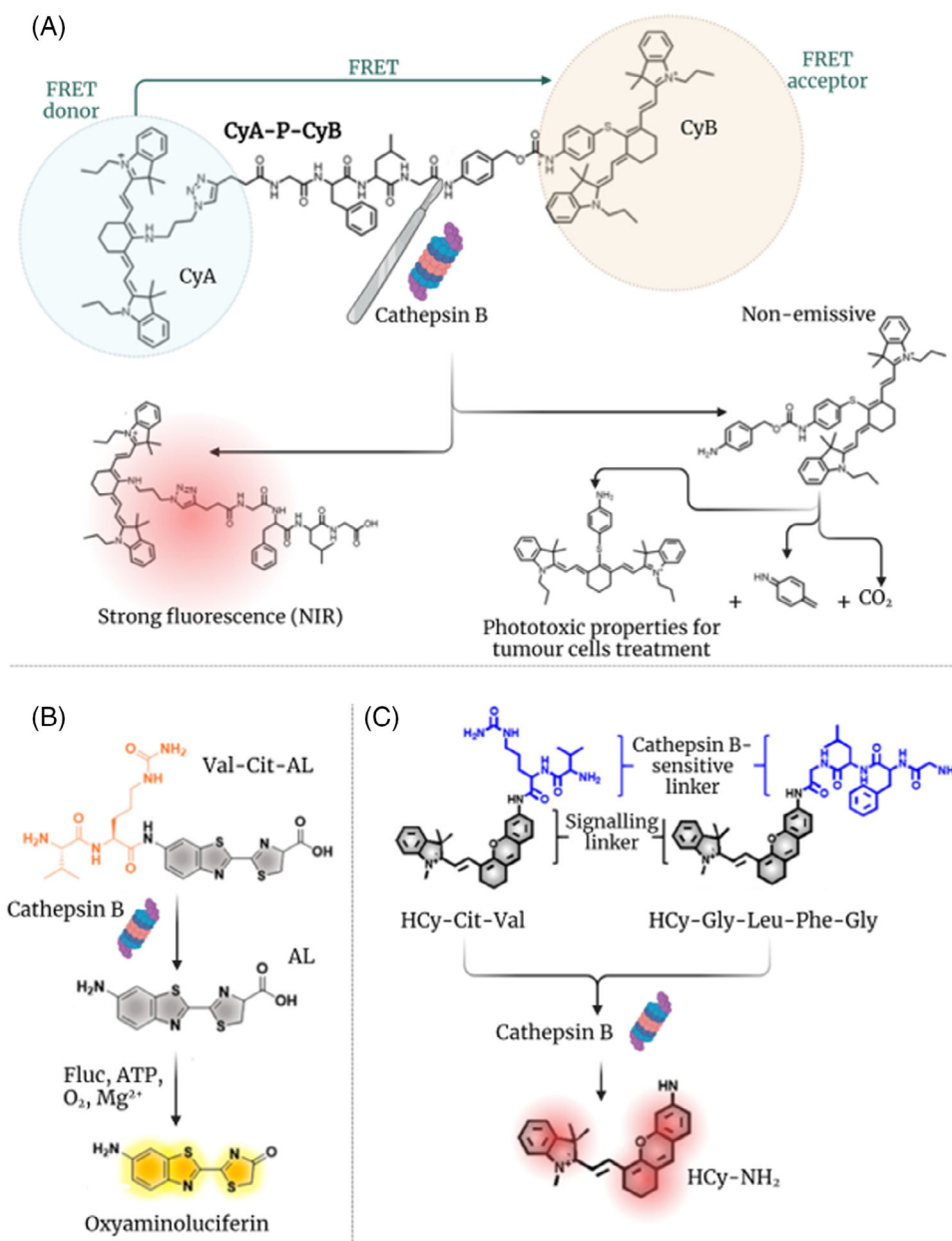


**FIGURE 7** (A) Illustration of the mechanism of action of CyA-P-CyB for both NIR AIE-activated cathepsin B detection and photodynamic therapy (PDT). The fluorescent molecule is composed of a FRET donor (CyA) and a FRET acceptor (CyB) component. The separation between these two components that occurs via the cleavage of the peptide linker in CyA-P-CyB by cathepsin B, results in the development of two components. The first component CyA has fluorescent properties, and the second component (Cy-S-Ph-NH<sub>2</sub>) has a PDT effect with strong phototoxicity to tumour cells.<sup>[108]</sup> Adapted with permission.<sup>[108]</sup> Copyright 2017, Elsevier. (B) Schematic illustration of the cleavage of Val-Cit-AL molecule by cathepsin B leading to the formation of oxyaminoluciferin with bioluminescence “turn-on” characteristics.<sup>[109]</sup> Adapted with permission.<sup>[109]</sup> Copyright 2019, American Chemical Society. (C) Schematic illustration of the cleavage of HCy-Cit-Val or HCy-Gly-Leu-Phe-Gly by cathepsin B.<sup>[110]</sup> Adapted with permission.<sup>[110]</sup> Copyright 2021, American Chemical Society.

(BODIPY) to bisphosphonate-targeting risedronate ligands (Figure 8B). With excellent fluorescent properties, the biomarker enabled the measurement of pH variation associated with osteoclast activity and investigated the mechanism of bone resorption in bone tissues.<sup>[115–117]</sup> These studies demonstrated that AIE biomarkers with high bone-binding affinities are suitable for analysing the effect of osteoclast activities on the surface of the bone, as their strong bone-binding alendronate fragments limited deep penetration. Optimising the strength of bonds between the biomarker and bone was shown to facilitate deep tissue penetration to explore the effect of osteolysis.

As mentioned previously, aggregation-caused quenching (ACQ) has been used to develop biomarkers for detecting molecular effectors such as TNF- $\alpha$ . However, this

approach may imply limitations in expanding the application of biomarkers specifically for implant failure detection. To overcome these limitations, employing efficient ACQ-AIE conversion approaches can synthesize more effective AIEgens with a broader application spectrum. This strategy may include introducing functional groups onto the molecule’s backbone, enhancing the molecule’s planarity and rigidity, and utilizing self-assembly, supramolecular interactions, and host–guest chemistry.<sup>[128]</sup>

In addition to the abovementioned strategies, future directions for the use of AIE biomarkers for early detection of bone loss could involve several innovative approaches and advancements. Researchers should focus on designing AIE biomarkers that specifically target biomarkers associated with bone loss, such as osteocalcin or collagen degradation

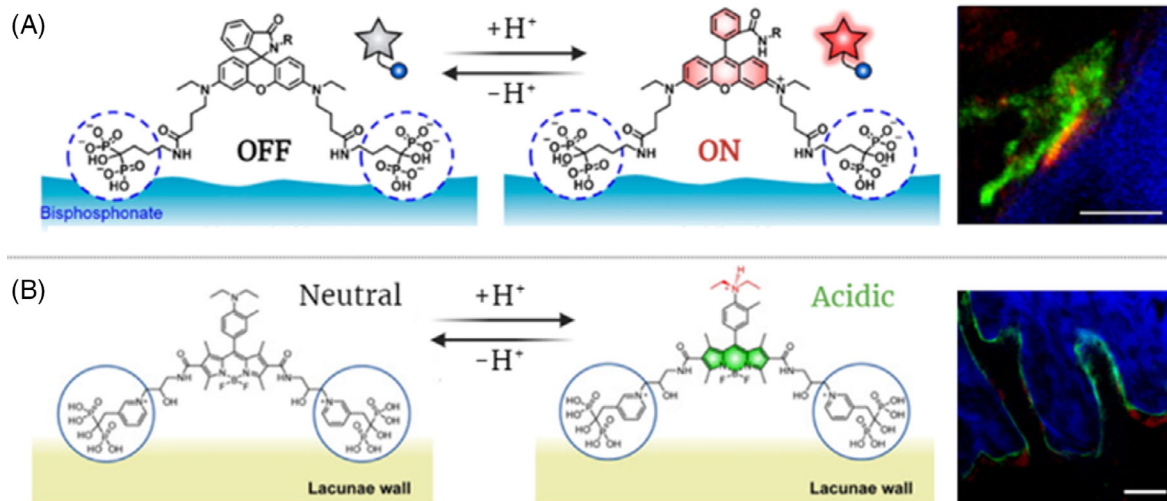


**FIGURE 8** (A) Detection of the acidic region in bone using Red-pHoc, a pH-sensitive biomarker with red fluorescence characteristics including two-photon excitation imaging captured from mouse bone tissue (scale bar = 50  $\mu\text{m}$ ).<sup>[111]</sup> Adapted with permission.<sup>[111]</sup> Copyright 2019, American Chemical Society. (B) The protonation of the diethylamino nitrogen atom of the BODIPY fluorophore leading to fluorescence activity, including two-photon excitation imaging captured from the mouse bone tissue (scale bar = 50  $\mu\text{m}$ ). For both (A) and (B), the excitation wavelength was 940 nm with the blue signals representing collagen in the bone matrix.<sup>[102]</sup> Adapted with permission.<sup>[102]</sup> Copyright 2020, John Wiley and Sons.

**TABLE 2** The contribution of key molecular effectors to the pathogenesis of osteolysis.

Molecular effectors	Contribution to osteolysis
RANKL, <sup>[129]</sup> IL-1, <sup>[66]</sup> and TNF- $\alpha$ <sup>[129]</sup>	Inhibiting osteoclast apoptosis
TNF- $\alpha$ , <sup>[66]</sup> IL-1, <sup>[66,130]</sup> and IL-6 <sup>[131]</sup>	Increasing RANKL expression
TNF- $\alpha$ , <sup>[68]</sup> and IL-1, <sup>[130]</sup> TLR <sup>[132–134]</sup>	Osteoclastogenesis augmentation
TNF- $\alpha$ <sup>[135]</sup>	Inhibiting procollagen I expression
TNF- $\alpha$ <sup>[130]</sup>	Increasing IL-1 and IL-1R expression
IL-1, <sup>[136]</sup> IL-6, <sup>[137]</sup> IL-18, <sup>[136]</sup> and TNF- $\alpha$ <sup>[130,136]</sup>	Activating MAPK and NF- $\kappa\text{B}$
IL-6 <sup>[15]</sup>	Stimulating TNF- $\alpha$
NALP3 inflammasome <sup>[134,136–139]</sup>	Activating cathepsin and ROS
Caspase-1 <sup>[136,137]</sup>	Activating pro-IL- $\beta$ and pro-IL-18
MMPs 1, 2, 3, 9, 10, 12 <sup>[140,141]</sup>	Degradation of periprosthetic ECM

products. These biomarkers would enable highly selective detection of bone degradation, enhancing the accuracy of early diagnosis. The detection of the osteolysis process which leads to implant loosening and failure should be the focus of new AIE biomarkers development. We have identified a list of key molecular effectors, including their biological pathways, that contribute to the osteolysis process (Table 2). The detection of these molecular effectors, using AIE biomarkers, may be relevant to the detection of implant loosening via monitoring of RANKL, IL-1, IL-1R and collagen (type I) expression, TNF- $\alpha$  stimulation, and degradation of periprosthetic extracellular matrix as well as the detection of osteoclast apoptosis and the activation of cathepsin.

Several studies have integrated AIEgens or traditional dyes to develop new fluorescent probes for detecting TNF- $\alpha$  and MMP13.<sup>[99,100,79,80]</sup> However, none of them have been used to directly detect molecular effectors originating from osteoclastogenesis and osteogenesis that lead to implant failure.

Therefore, exploring the application of existing probes for the early detection of implant failure is another strategy to consider. Additionally, the detection of urinary N-terminal telopeptide using AIEgens has been overlooked. Given the clinical relevance of this molecular effector, it is important to focus attention on this area.

Multiplexed AIE biomarker systems could be developed to detect multiple biomarkers simultaneously, providing a comprehensive assessment of bone health. By incorporating multiple AIE probes with distinct emission wavelengths, researchers could create multiplexed imaging platforms capable of detecting various indicators of bone loss in a single assay. This strategy has been utilized to develop advanced point-of-care biosensing systems using AIEgens and could be expanded to address joint replacement issues. Advancements in imaging technologies could enable non-invasive, real-time monitoring of bone health using AIE probes. Researchers could explore the development of AIE-based imaging techniques, such as fluorescence lifetime imaging or multispectral imaging, for in vivo assessment of bone integrity and early detection of pathological changes. AIE probes could be integrated into biomaterials or implantable devices for continuous monitoring of bone health. By incorporating AIE probes into orthopaedic implants or scaffolds, clinicians could monitor bone regeneration processes and detect early signs of implant failure or bone loss, facilitating timely intervention and treatment. There is potential for the development of point-of-care diagnostic devices based on AIE probes for rapid and cost-effective screening of bone health. Miniaturised AIE-based diagnostic platforms could be designed for use in clinical settings or remote locations, enabling early detection of bone loss and facilitating timely management of skeletal disorders including bone loss and implant failure.

## 8 | CONCLUSION

The increasing number of joint replacements for degenerative joint disease highlights the urgent need for effective early detection methods for implant failure. Current clinical

practices are insufficient for the early identification of implant issues, and biomarkers for early detection of joint implant failure have not been fully utilized. Unfortunately, the development and application of AIEgens for monitoring and detecting molecular effectors involved in osteogenesis and osteoclastogenesis processes have been significantly overlooked. Specifically, there are no AIEgens currently available for targeting, detecting, and monitoring the activity of key molecular effectors such as cathepsin K, N-terminal telopeptide, and osteocalcin. Additionally, a few AIEgens have recently been developed to detect a limited range of such molecular effectors (e.g., TNF- $\alpha$  and MMP13), which do not originate from osteoclastogenesis or osteogenesis. Consequently, their application for early detection of joint implant failure remains unexplored. The strategies outlined in this review are among the many needed to advance the field and enhance the clinical use of AIEgens in this critical area. It is important to note that this systematic mapping review<sup>[142]</sup> is crucial for identifying gaps in the research literature and categorizing existing studies, which is central to the commissioning of further primary research that is currently lacking.

## ACKNOWLEDGEMENTS

The authors have nothing to report.

## CONFLICT OF INTEREST STATEMENT

The authors declare no conflicts of interest.

## ORCID

Javad Tavakoli  <https://orcid.org/0000-0002-0696-6530>

Qi Hu  <https://orcid.org/0000-0003-4315-6665>

Youhong Tang  <https://orcid.org/0000-0003-2718-544X>

## REFERENCES

1. S. Kurtz, K. Ong, E. Lau, F. Mowat, M. Halpern, *J. Bone Joint Surg. Am.* **2007**, *89*, 780.
2. S. M. Kurtz, E. Lau, K. Ong, K. Zhao, M. Kelly, K. J. Bozic, *Clin. Orthop. Relat. Res.* **2009**, *467*, 2606.
3. M. D. Jones, C. L. Buckle, *Orthop. Trauma* **2020**, *34*, 146.
4. R. M. Bhalekar, S. R. Wells, M. E. Nargol, S. Shariatpanahi, A. V. Nargol, S. Waller, L. Wildberg, S. Tilley, D. J. Langton, *Knee* **2024**, *47*, 1.
5. N. Athanasou, *Bone Joint Res.* **2016**, *5*, 162.
6. A. M. Kandahari, X. Yang, K. A. Laroche, A. S. Dighe, D. Pan, Q. Cui, *Bone Res.* **2016**, *4*, 16014.
7. Y. Yang, D. Sheng, J. Shi, L. Xiao, Z. Wang, Z. Yin, Q. Zhuang, S. Chen, Y. Li, Y. Gu, *Biomed. Pharmacother.* **2023**, *158*, 114113.
8. A. J. Kievit, G. S. Buijs, J. G. Dobbe, A. Ter Wee, G. M. Kerckhoffs, G. J. Streekstra, M. U. Schafroth, L. Blankevoort, *Clin. Biomech.* **2023**, *104*, 105930.
9. S. D. Stegelmann, R. Rahmani, M. Tille, S. Eaddy, S. Phillips, *J. Orthop.* **2023**, *45*, 37.
10. L. M. Childs, J. J. Goater, R. J. O'Keefe, E. M. Schwarz, *J. Bone Miner. Res.* **2001**, *16*, 338.
11. B. Yu, S. Hao, S. Sun, H. Guo, X. Yang, X. Ma, Q. Jin, *Zhongguo XiuFu Chongjian Waike Zazhi* **2013**, *27*, 994.
12. H. Guo, J. Zhang, S. Hao, Q. Jin, *Int. J. Mol. Med.* **2013**, *32*, 296.
13. E. Tsourdi, K. Jähn, M. Rauner, B. Busse, L. F. Bonewald, *J. Musculoskeletal Neuronal Interact.* **2018**, *18*, 292.
14. S. Noordin, B. Masri, *Can. J. Surg.* **2012**, *55*, 408.
15. Y. Jiang, T. Jia, P. H. Wooley, S. Y. Yang, *Acta Orthop. Belg.* **2013**, *79*, 23547507.
16. P. E. Purdue, A. S. Levin, K. Ren, T. P. Sculco, D. Wang, S. R. Goldring, *HSS J.* **2013**, *9*, 79.
17. R. Supra, D. K. Agrawal, *J. Orthop. Sports Med.* **2023**, *5*, 9.
18. W. J. Boyle, W. S. Simonet, D. L. Lacey, *Nature* **2003**, *423*, 337.
19. P. Skládal, Z. Jílková, I. Svoboda, V. Kolář, *Biosens. Bioelectron.* **2005**, *20*, 2027.
20. M. Ramanathan, M. Patil, R. Epur, Y. Yun, V. Shanov, M. Schulz, W. R. Heineman, M. K. Datta, P. N. Kumta, *Biosens. Bioelectron.* **2016**, *77*, 580.
21. E. Kozhevnikov, S. Qiao, F. Han, W. Yan, Y. Zhao, X. Hou, A. Acharya, Y. Shen, H. Tian, H. Zhang, X. Chen, Y. Zheng, H. Yan, M. Guo, W. Tian, *Biosens. Bioelectron.* **2019**, *141*, 111481.
22. S. Krishnamoorthy, A. A. Iliadis, T. Bei, G. P. Chrousos, *Biosens. Bioelectron.* **2008**, *24*, 313.
23. S. Krishnamoorthy, T. Bei, E. Zoumakis, G. P. Chrousos, A. A. Iliadis, *Biosens. Bioelectron.* **2006**, *22*, 707.
24. W. Grellner, *Forensic Sci. Int.* **2002**, *130*, 90.
25. E. Sánchez-Tirado, C. Salvo, A. González-Cortés, P. Yáñez-Sedeño, F. Langa, J. M. Pingarrón, *Anal. Chim. Acta* **2017**, *959*, 66.
26. S. K. Arya, P. Estrela, *Methods* **2017**, *116*, 125.
27. H. He, Y. Yuan, W. Wang, N.-R. Chiou, A. J. Epstein, L. J. Lee, *Biomicrofluidics* **2009**, *3*, 022401.
28. K. Freeman, M. Connock, P. Auguste, S. Taylor-Phillips, H. Mistry, D. Shyangdan, R. P. Arasaradnam, P. Sutcliffe, A. Clarke, *Health Technol. Assess.* **2016**, *20*, 1.
29. M. Taniguchi, K. Nagaoka, T. Kunikata, T. Kayano, H. Yamauchi, S. Nakamura, M. Ikeda, K. Orita, M. Kurimoto, *J. Immunol. Methods* **1997**, *206*, 107.
30. F. Battaglia, F. Torrini, P. Palladino, S. Scarano, M. Minunni, *Biosens. Bioelectron.* **2023**, *242*, 115713.
31. A. D. Buskermolen, C. M. S. Michielsen, A. M. de Jong, M. W. J. Prins, *Biosens. Bioelectron.* **2024**, *249*, 115934.
32. M. Qi, Y. Zhang, C. Cao, M. Zhang, S. Liu, G. Liu, *Anal. Chem.* **2016**, *88*, 9614.
33. H. Gao, X. Wang, M. Li, H. Qi, Q. Gao, C. Zhang, *ACS Appl. Bio Mater.* **2019**, *2*, 3052.
34. Q. Cai, H. Li, W. Dong, G. Jie, *Biosens. Bioelectron.* **2023**, *241*, 115704.
35. H. Hu, D. Pan, H. Xue, M. Zhang, Y. Zhang, Y. Shen, *J. Electroanal. Chem.* **2018**, *824*, 195.
36. A. K. Yagati, M.-H. Lee, J. Min, *Bioelectrochemistry* **2018**, *122*, 93.
37. W. Wei, Z. Qiu, *Biosens. Bioelectron.* **2022**, *217*, 114670.
38. H. Li, H. Lin, W. Lv, P. Gai, F. Li, *Biosens. Bioelectron.* **2020**, *165*, 112336.
39. L. Lin, Y. Hu, L. Zhang, Y. Huang, S. Zhao, *Biosens. Bioelectron.* **2017**, *94*, 523.
40. J. Mei, Y. Hong, J. W. Lam, A. Qin, Y. Tang, B. Z. Tang, *Adv. Mater.* **2014**, *26*, 5429.
41. Y. Zhou, J. Hua, D. Ding, Y. Tang, *Biomaterials* **2022**, *286*, 121605.
42. X. Zhang, B. Yao, Q. Hu, Y. Hong, A. Wallace, K. Reynolds, C. Ramsey, A. Maeder, R. Reed, Y. Tang, *Mater. Chem. Front.* **2020**, *4*, 2548.
43. J. Tavakoli, S. Pye, A. M. Reza, N. Xie, J. Qin, C. L. Raston, B. Z. Tang, Y. Tang, *Mater. Chem. Front.* **2020**, *4*, 537.
44. J. Tavakoli, N. Joseph, C. L. Raston, Y. Tang, *Nanoscale Adv.* **2020**, *2*, 633.
45. J. Tavakoli, N. Joseph, C. Chuah, C. L. Raston, Y. Tang, *Mater. Chem. Front.* **2020**, *4*, 2126.
46. W. Wu, M. Shen, X. Liu, L. Shen, X. Ke, W. Li, *Biosens. Bioelectron.* **2020**, *150*, 111912.
47. J. Chang, H. Li, T. Hou, W. Duan, F. Li, *Biosens. Bioelectron.* **2018**, *104*, 152.
48. H. Guan, W. Wang, Z. Jiang, B. Zhang, Z. Ye, J. Zheng, W. Chen, Y. Liao, Y. Zhang, *Adv. Mater.* **2024**, *36*, 2312081.
49. B. Cai, J. Dong, B. Su, Q. Yang, C. Wang, L. Yang, Z. Song, J. Liu, R. Jin, Y. Li, *Adv. Funct. Mater.* **2024**, *34*, 2312260.
50. X. Zhang, X. Liu, H. Yu, S. Shen, J. Zhi, Z. Gao, J. Xin, J. Song, L. Shao, C. Meng, F. An, T. Huo, S. Liu, Y. Zhang, L. Xu, G. Li, *Aggregate* **2023**, *4*, e381.
51. Z. Zhao, Z. Wang, J. Tavakoli, G. Shan, J. Zhang, C. Peng, Y. Xiong, X. Zhang, T. S. Cheung, Y. Tang, B. Huang, Z. Yu, J. W. Y. Lam, B. Z. Tang, *Aggregate* **2021**, *2*, e36.
52. Z. Song, Y. Hong, R. T. Kwok, J. W. Lam, B. Liu, B. Z. Tang, *J. Mater. Chem. B* **2014**, *2*, 1717.
53. M. Zhao, Y. Gao, S. Ye, J. Ding, A. Wang, P. Li, H. Shi, *Analyst* **2019**, *144*, 6262.
54. X. Cai, C. J. Zhang, F. Ting Wei Lim, S. J. Chan, A. Bandla, C. K. Chuan, F. Hu, S. Xu, N. V. Thakor, L. D. Liao, *Small* **2016**, *12*, 6576.

55. M. Gao, J. Chen, G. Lin, S. Li, L. Wang, A. Qin, Z. Zhao, L. Ren, Y. Wang, B. Z. Tang, *ACS Appl. Mater. Interfaces* **2016**, *8*, 17878.
56. M. Gao, Y. Li, X. Chen, S. Li, L. Ren, B. Z. Tang, *ACS Appl. Mater. Interfaces* **2018**, *10*, 14410.
57. X. Wang, P. Chen, H. Yang, J. Liu, R. Tu, H.-T. Feng, H. Dai, *ACS Appl. Mater. Interfaces* **2023**, *15*, 25382.
58. X. Han, Y. Ma, Y. Chen, X. Wang, Z. Wang, *Anal. Chem.* **2020**, *92*, 2830.
59. J. Chen, L. Chen, Z. She, F. Zeng, S. Wu, *Aggregate* **2024**, *5*, e419.
60. W. Wang, G. Zhang, Z. Chen, H. Xu, B. Zhang, R. Hu, A. Qin, Y. Hua, *Bio-Des. Manuf.* **2023**, *6*, 704.
61. Y. Zhang, X. Kang, J. Li, J. Song, X. Li, W. Li, J. Qi, *ACS Nano* **2024**, *18*, 2231.
62. M. T. Mertens, J. A. Singh, *Open Orthop. J.* **2011**, *5*, 92.
63. D. R. Sumner, R. Ross, E. Purdue, *Clin. Orthop. Relat. Res.* **2014**, *472*, 3728.
64. S. Hasan, P. van Schie, B. L. Kaptein, J. W. Schoones, P. J. Marang-van de Mheen, R. G. Nelissen, *EFORT Open Rev.* **2024**, *9*, 25.
65. S. Goodman, E. Gibon, J. Pajarinen, T.-H. Lin, M. Keeney, P.-G. Ren, C. Nich, Z. Yao, K. Egashira, F. Yang, *J. R. Soc., Interface* **2014**, *11*, 20130962.
66. L. C. Hofbauer, M. Schoppet, *JAMA, J. Am. Med. Assoc.* **2004**, *292*, 490.
67. R. B. Kimble, S. Srivastava, F. P. Ross, A. Matayoshi, R. Pacifici, *J. Biol. Chem.* **1996**, *271*, 28890.
68. J. Lam, S. Takeshita, J. E. Barker, O. Kanagawa, F. P. Ross, S. L. Teitelbaum, *J. Clin. Invest.* **2000**, *106*, 1481.
69. A. S. Shanbhag, C. T. Hasselman, H. E. Rubash, *Clin. Orthop. Relat. Res.* **1997**, *344*, 4.
70. J. Pajarinen, T. Lin, E. Gibon, Y. Kohno, M. Maruyama, K. Nathan, L. Lu, Z. Yao, S. B. Goodman, *Biomaterials* **2019**, *196*, 80.
71. A. Insua, A. Monje, H. L. Wang, R. J. Miron, *J. Biomed. Mater. Res., Part A* **2017**, *105*, 2075.
72. T. R. Green, J. Fisher, J. B. Matthews, M. H. Stone, E. Ingham, *J. Biomed. Mater. Res.* **2000**, *53*, 490.
73. L. Gilbert, X. He, P. Farmer, S. Boden, M. Kozlowski, J. Rubin, M. S. Nanes, *Endocrinology* **2000**, *141*, 3956.
74. M. A. Terkawi, G. Matsumae, T. Shimizu, D. Takahashi, K. Kadoya, N. Iwasaki, *Int. J. Mol. Sci.* **2022**, *23*, 1786.
75. M. Panasiuk, M. Synder, M. Drynkowska-Panasiuk, O. Bończak, *Chir. Narzadow Ruchu Ortop. Pol.* **2006**, *71*, 261.
76. E. Anitua, M. H. Alkhraisat, A. Eguia, *Cureus* **2023**, *15*, e33237.
77. N. Cobelli, B. Scharf, G. M. Crisi, J. Hardin, L. Santambrogio, *Nat. Rev. Rheumatol.* **2011**, *7*, 600.
78. Z. Zheng, T. Zhou, R. Hu, M. Huang, X. Ao, J. Chu, T. Jiang, A. Qin, Z. Zhang, *Bioact. Mater.* **2020**, *5*, 1018.
79. J. Li, C. W. T. Leung, D. S. H. Wong, J. Xu, R. Li, Y. Zhao, C. Y. Y. Yung, E. Zhao, B. Z. Tang, L. Bian, *ACS Appl. Mater. Interfaces* **2019**, *11*, 22074.
80. R. Yan, Y. Guo, X. Wang, G. Liang, A. Yang, J. Li, *ACS Nano* **2022**, *16*, 8399.
81. F.-Y. Cao, Y. Long, S.-B. Wang, B. Li, J.-X. Fan, X. Zeng, X.-Z. Zhang, *J. Mater. Chem. B* **2016**, *4*, 4534.
82. J. Liang, R. T. K. Kwok, H. Shi, B. Z. Tang, B. Liu, *ACS Appl. Mater. Interfaces* **2013**, *5*, 8784.
83. Y. Tan, L. Zhang, K. H. Man, R. Peltier, G. Chen, H. Zhang, L. Zhou, F. Wang, D. Ho, S. Q. Yao, Y. Hu, H. Sun, *ACS Appl. Mater. Interfaces* **2017**, *9*, 6796.
84. F. Zheng, S. Guo, F. Zeng, J. Li, S. Wu, *Anal. Chem.* **2014**, *86*, 9873.
85. Z. Song, R. T. K. Kwok, E. Zhao, Z. He, Y. Hong, J. W. Y. Lam, B. Liu, B. Z. Tang, *ACS Appl. Mater. Interfaces* **2014**, *6*, 17245.
86. M. M. Mohamed, B. F. Sloane, *Nat. Rev. Cancer* **2006**, *6*, 764.
87. K. A. Schleyer, L. Cui, *Org. Biomol. Chem.* **2021**, *19*, 6182.
88. Y. T. Konttinen, M. Takagi, J. Mandelin, J. Lassus, J. Salo, M. Ainola, T.-F. Li, I. Virtanen, M. Liljestrom, H. Sakai, Y. Kobayashi, T. Sorsa, R. Lappalainen, A. Demulder, S. Santavirta, *J. Bone Miner. Res.* **2001**, *16*, 1780.
89. R. A. Dodds, I. E. James, D. Rieman, R. Ahern, S. M. Hwang, J. R. Connor, S. D. Thompson, D. F. Veber, F. H. Drake, S. Holmes, *J. Bone Miner. Res.* **2001**, *16*, 478.
90. Y. Yuan, C. J. Zhang, M. Gao, R. Zhang, B. Z. Tang, B. Liu, *Angew. Chem., Int. Ed.* **2015**, *54*, 1780.
91. P. Chen, F. Qu, L. He, M. Li, P. Sun, Q. Fan, C. Zhang, D. Li, *J. Nanobiotechnol.* **2023**, *21*, 230.
92. D. M. Lapierre, N. Tanabe, A. Pereverzev, M. Spencer, R. P. Shugg, S. J. Dixon, S. M. Sims, *J. Biol. Chem.* **2010**, *285*, 25792.
93. N. Fontaine, L. Harter, A. Murette, D. Boudreau, *ACS Omega* **2022**, *8*, 1067.
94. S. Sri, G. Lakshmi, P. Gulati, D. Chauhan, A. Thakkar, P. R. Solanki, *Anal. Chim. Acta* **2021**, *1182*, 338909.
95. M. L. Yola, N. Atar, *Anal. Bioanal. Chem.* **2021**, *413*, 2481.
96. L. Yang, A. Hou, S. Wang, J. Zhang, W. Man, X. Guo, B. Yang, Q. Wang, H. Jiang, H. Kuang, *Anal. Biochem.* **2020**, *596*, 113643.
97. S. Noh, H. Lee, J. Kim, H. Jang, J. An, C. Park, M.-H. Lee, T. Lee, *Biosens. Bioelectron.* **2022**, *207*, 114159.
98. Z. Sun, L. Deng, H. Gan, R. Shen, M. Yang, Y. Zhang, *Biosens. Bioelectron.* **2013**, *39*, 215.
99. H. Li, X. Li, L. Chen, B. Li, H. Dong, H. Liu, X. Yang, H. Ueda, J. Dong, *ACS Omega* **2021**, *6*, 31009.
100. H. Yun, H. Ueda, H.-J. Jeong, *Biotechnol. Bioprocess Eng.* **2022**, *27*, 846.
101. N. Talapphet, C. S. Huh, M.-M. Kim, *J. Immunol. Methods* **2024**, *527*, 113648.
102. R. Abe, H.-J. Jeong, D. Arakawa, J. Dong, H. Ohashi, R. Kaigome, F. Saiki, K. Yamane, H. Takagi, H. Ueda, *Sci. Rep.* **2014**, *4*, 4640.
103. C.-I. Chung, R. Makino, Y. Ohmuro-Matsuyama, H. Ueda, *J. Biosci. Bioeng.* **2017**, *123*, 272.
104. J. Dong, C. Miyake, T. Yasuda, H. Oyama, I. Morita, T. Tsukahara, M. Takahashi, H.-J. Jeong, T. Kitaguchi, N. Kobayashi, H. Ueda, *Biosens. Bioelectron.* **2020**, *165*, 112425.
105. R. M. Clegg, *Fluorescence resonance energy transfer. Curr. Opin. Biotechnol.* **1995**, *6*, 103.
106. R. M. Clegg, *Lab. Tech. Biochem. Mol. Biol.* **2009**, *33*, 1.
107. B. Liu, B. Wang, Z. Wang, Y. Meng, Y. Li, L. Li, J. Wang, M. Zhai, R. Liu, F. Wei, *ACS Appl. Mater. Interfaces* **2023**, *15*, 43503.
108. X. Chen, D. Lee, S. Yu, G. Kim, S. Lee, Y. Cho, H. Jeong, K. T. Nam, J. Yoon, *Biomaterials* **2017**, *122*, 130.
109. Y. Ni, Z. Hai, T. Zhang, Y. Wang, Y. Yang, S. Zhang, G. Liang, *Anal. Chem.* **2019**, *91*, 14834.
110. X. Chen, X. Ren, Y. Zhu, Z. Fan, L. Zhang, Z. Liu, L. Dong, Z. Hai, *Anal. Chem.* **2021**, *93*, 9304.
111. M. Minoshima, J. Kikuta, Y. Omori, S. Seno, R. Suehara, H. Maeda, H. Matsuda, M. Ishii, K. Kikuchi, *ACS Cent. Sci.* **2019**, *5*, 1059.
112. C. Liu, C. Sun, H. Huang, K. Janda, T. Edgington, *Cancer Res.* **2003**, *63*, 2957.
113. Y. Yuan, S. Ge, H. Sun, X. Dong, H. Zhao, L. An, J. Zhang, J. Wang, B. Hu, G. Liang, *ACS Nano* **2015**, *9*, 5117.
114. Y. Cui, W. Du, G. Liang, *ChemNanoMat* **2016**, *2*, 344.
115. R. Hashimoto, M. Minoshima, J. Kikuta, S. Yari, S. D. Bull, M. Ishii, K. Kikuchi, *Angew. Chem. Int. Ed.* **2020**, *59*, 20996.
116. H. Maeda, T. Kowada, J. Kikuta, M. Furuya, M. Shirazaki, S. Mizukami, M. Ishii, K. Kikuchi, *Nat. Chem. Biol.* **2016**, *12*, 579.
117. T. Kowada, J. Kikuta, A. Kubo, M. Ishii, H. Maeda, S. Mizukami, K. Kikuchi, *J. Am. Chem. Soc.* **2011**, *133*, 17772.
118. E. Mijiritsky, L. Ferroni, C. Gardin, O. Peleg, A. Gultekin, A. Saglanmak, L. G. Delogu, D. Mitrecic, A. Piattelli, M. Tatullo, B. Zavan, *J. Clin. Med.* **2020**, *9*, 38.
119. W. Chen, Z. Li, Y. Guo, Y. Zhou, Z. Zhang, Y. Zhang, G. Luo, X. Yang, W. Liao, C. Li, *Cell. Physiol. Biochem.* **2015**, *35*, 1857.
120. G. Luo, Z. Li, Y. Wang, H. Wang, Z. Zhang, W. Chen, Y. Zhang, Y. Xiao, C. Li, Y. Guo, P. Sheng, *Inflammation* **2016**, *39*, 775.
121. M. J. Steinbeck, L. J. Jablonowski, J. Parvizi, T. A. Freeman, *J. Arthroplasty* **2014**, *29*, 843.
122. S. A. Syggelos, A. J. Aletras, I. Smirlaki, S. S. Skandalis, *Biomed. Res. Int.* **2013**, *2013*, 230805.
123. F. Qu, Q. Yang, B. Wang, J. You, *Talanta* **2020**, *207*, 120289.
124. Y.-X. Liang, X.-Y. Sun, D.-Z. Xu, J.-R. Huang, Q. Tang, Z.-L. Lu, R. Liu, *Bioorg. Chem.* **2022**, *119*, 105559.
125. X. He, Y. Luo, Y. Li, Y. Pan, R. T. K. Kwok, L. He, X. Duan, P. Zhang, A. Wu, B. Z. Tang, J. Li, *Aggregate* **2024**, *5*, e396.
126. A. Lao, J. Wu, D. Li, A. Shen, Y. Li, Y. Zhuang, K. Lin, J. Wu, J. Liu, *Small* **2023**, *19*, 2206919.
127. H. Cao, Y. Yang, J. Li, *Aggregate* **2020**, *1*, 69.
128. W. Zhu, L. Huang, C. Wu, L. Liu, H. Li, *Luminescence* **2024**, *39*, e4655.
129. S. E. Lee, W. J. Chung, H. B. Kwak, C. H. Chung, K. B. Kwack, Z. H. Lee, H. H. Kim, *J. Biol. Chem.* **2001**, *276*, 49343.

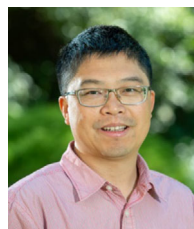
130. S. Wei, H. Kitaura, P. Zhou, F. P. Ross, S. L. Teitelbaum, *J. Clin. Invest.* **2005**, *115*, 282.
131. F. Yoshitake, S. Itoh, H. Narita, K. Ishihara, S. Ebisu, *J. Biol. Chem.* **2008**, *283*, 11535.
132. A. M. Kandahari, X. Yang, A. S. Dighe, D. Pan, Q. Cui, *J. Immunol. Res.* **2015**, *2015*, 192415.
133. R. Maitra, C. C. Clement, G. M. Crisi, N. Cobelli, L. Santambrogio, *PLoS One* **2008**, *3*, e2438.
134. R. Maitra, C. C. Clement, B. Scharf, G. M. Crisi, S. Chitta, D. Paget, P. E. Purdue, N. Cobelli, L. Santambrogio, *Mol. Immunol.* **2009**, *47*, 175.
135. C. Vermes, K. A. Roebuck, R. Chandrasekaran, J. G. Dobai, J. J. Jacobs, T. T. Glant, *J. Bone Miner. Res.* **2000**, *15*, 1756.
136. M. Lamkanfi, V. M. Dixit, *Immunol. Rev.* **2009**, *227*, 95.
137. N. Cobelli, B. Scharf, G. M. Crisi, J. Hardin, L. Santambrogio, *Nat. Rev. Rheumatol.* **2011**, *7*, 600.
138. S. L. Cassel, S. C. Eisenbarth, S. S. Iyer, J. J. Sadler, O. R. Colegio, L. A. Tephly, A. B. Carter, P. B. Rothman, R. A. Flavell, F. S. Sutterwala, *Proc. Natl. Acad. Sci. U. S. A.* **2008**, *105*, 9035.
139. L. A. O'Neill, *Science* **2008**, *320*, 619.
140. I. Takei, M. Takagi, S. Santavirta, H. Ida, M. Ishii, T. Ogino, M. Ainola, Y. T. Konttinen, *J. Biomed. Mater. Res.* **2000**, *52*, 613.
141. M. Takagi, Y. T. Konttinen, S. Santavirta, T. Sorsa, A. Z. Eisen, L. Nordsletten, A. Suda, *Acta Orthop. Scand.* **1994**, *65*, 281.
142. M. J. Grant, A. Booth, *Health Inf. Libr. J.* **2009**, *26*, 91.

**How to cite this article:** J. Tavakoli, Q. Hu, J. L. Tipper, Y. Tang, *Aggregate* **2024**, *5*, e645.  
<https://doi.org/10.1002/agt2.645>

## AUTHOR BIOGRAPHIES



**Javad Tavakoli** is an associate professor at RMIT University in Melbourne, Australia. His research focuses on using additive manufacturing and nanofabrication to engineer 3D tissue organ models, organ-on-a-chip platforms and implants for orthopaedic applications. Additionally, he employs mechanistic multi-scale approaches to develop research toolboxes for various orthopaedic purposes. He is also interested in aggregation-induced emission biomarkers for biomedical applications.



**Youhong Tang** is a Matthew Flinders professor of Engineering at Flinders University. Currently, he is a research leader at the Institute for NanoScale Science and Technology and a Management Committee in Medical Device Research Institute at Flinders University. His research interests mainly focus on structure-processing-property relationship of polymeric (nano) materials/composites for sustainability and chemo/ biosensors and their devices with aggregation-induced emission features.